PhD Dissertation

CO_2ENHANCED OIL RECOVERY BASED ON RESERVOIR COMPACTION, THERMAL MODELING, AND FORMATION DAMAGES

저류층압밀, 열모델링,
지층손상에기반한 CO2 증진오일회수

AUGUST 2014

SEOUL NATIONAL UNIVERSITY, GRADUATE SCHOOL
DEPARTMENT OF ENERGY SYSTEMSENGINEERING

Ilyas Khurshid

CO_2 ENHANCED OIL RECOVERY BASED ON RESERVOIR COMPACTION, THERMAL MODELING AND FORMATION DAMAGES

저류층 압밀, 열모델링, 지층손상에 기반한 CO_2 증진 오일회수

지도교수 최종근

이 논문을 공학박사 학위논문으로 제출함

2014 년 4 월

서울대학교 대학원
에너지시스템공학부
Ilyas Khurshid

Ilyas Khurshid 의 공학박사 학위논문을 인준함

2014 년 6 월

위 원장 박 해 충 (인)

부위원장 최 종 근 (인)

위 원 송 재 준 (인)

위 원 배 위 섭 (인)

위 원 신 현 동 (인)

ABSTRACT

Ilyas Khurshid
Department of Energy Systems Engineering
College of Engineering
Seoul National University

The primary objective of this dissertation is to develop new, simple, and robust methods and practices for enhance oil recovery (EOR) and CO_2 storage. For this purpose a step by step structure is developed, which will provide a good understanding of interrelationships between rock compaction and CO_2 injection time, CO_2 thermal modeling, CO_2 related formation damages, and methods to minimize these damages.

The first objective is to develop an analytical model using the concept of pore arrangement at macroscopic level. This model along with the proposed failure-line methodology determines a minimum reservoir pressure. This pressure represents the pressure after which permanent pore collapse will occur and it can be used to determine optimal time ranges for CO_2 injection. On the basis of detail analysis, an optimal CO_2 injection time ranges are to inject it before touching the failure line. This practice will enhance oil recovery and CO_2 storage.

The second objective is to determine CO_2 temperature profile in wellbore, factors affecting it, and formation damages caused due to heated CO_2. For this purpose a simulator is developed and experimental determined specific heat values of CO_2 are used to predict the temperature of CO_2. This approach results in accurate CO_2 temperature predictions, because the thermodynamic properties of CO_2 vary with temperature and pressure. From sensitivity analyses of CO_2 injection parameters, it is found that the injection rate, injection time, geothermal gradient, and surface temperature play a key role in controlling CO_2 temperature in sequestration activities.

When carbon dioxide enters in a reservoir, it may react with the formation leading to immense formation damages such as asphaltene deposition, rock dissolution, and particle precipitation. The third objective is to develop a simulator to model chemical reactivity, pH shift, asphaltene deposition, and particle dissolution and precipitation. It is found that these processes may lead to cementation and result in irreversible damages to the porous media. It is observed that this cementation depends on the amount and reactivity of asphaltene, and the reactivity of CO_2 with water and rock. It is also analyzed that substantial amount of cementations occurs for high injection rate and long injection period. From the sensitivity analysis, it is established that deep oil and gas reservoirs are better candidates for CO_2 sequestration than shallow reservoirs due to low formation damages.

The final objective of this study is to develop an integrated methodology to minimize asphaltene deposition, and to increase oil recovery and CO_2 storage. When CO_2 is injected at immiscible conditions, asphaltene deposition is low with less recovery. However, when the conditions are miscible, recovery increases but it also triggers asphaltene deposition. From detail simulation study, it is found that there are a number of minimum miscibility pressures (MMP), but three are important: near, at, and above MMP. For the first MMP there is high asphaltene deposition. When the pressure is at and above the MMP, the deposited asphaltene is removed from the reservoir, because CO_2 develops contact with asphaltene at high pressure leading to its redissolution and removal.

Key words: Reservoir compaction, Carbon dioxide injection, Optimal injection time ranges, Thermal modeling, and Formation damage.

Student ID: 2011-31311

TABLE OF CONTENTS

LIST OF TABLES

LIST OF FIGURES

Chapter 1

INTRODUCTION AND OVERVIEW

1.1 Backgrounds

Energy demand is ever increasing and growing throughout the world. This use of energy for development comes with carbon dioxide (CO_2) emission, which is accepted globally as a major cause of climate change. IPCC (2005) has mentioned that the concentration of CO_2 in pre industrial times was just 280 ppm and now it has increased to 401.14 ppm (Tans and Keeling, 2014). During the last century, the average global temperature was 0.74 °C and it is increasing at an accelerated rate. It is estimated that by 2100, the average global temperature will be in range between 1.2-6.5 °C.

The climate change has observable, severe, and vulnerable effects on our environment. It has caused glaciers shrinking, loss of sea ice, accelerated sea level rise, increasing risk of drought, fire and floods, stronger storms and increased storm damage, economic loss, more intense heat waves, and heat related illness and disease. These climate changes and global warming, not only affect economic output but also shatter economic growth (IEA, 2012). Therefore, substantial reductions in CO_2 from power plant and other huge CO_2 emitting industries are required to manage the risks of climate change for sustainable development.

To reduce CO_2 emissions, it requires a fundamental change in the industry in the way of electricity generation, operations of industrial processes, and in methods of transportation. These changes include making the processes more energy efficient, switching to less carbon intensive, and to renewable energy sources. Possible renewable energy sources are geothermal, wind, solar, biomass, and tidal. However, the fossil fuels such as coal, oil, and gas are and will continue to be widely used and cannot be replaced (Global CCS Institute, 2012). Therefore, something must be done to reduce the emissions from these fossil fuels.

Carbon capture and storage (CCS) is a low-carbon technology and it has the potential to reduce CO_2 emissions and mitigate climate change. It is a technique to capture, transport, and store CO_2 in deep subsurface structures. Potential structures are depleted oil and gas reservoirs, coal seams, organic rich shales, and saline aquifers. Thus, CCS isolates CO_2 emissions from the atmosphere (IPCC, 2005; IEA, 2012; Global CCS Institute, 2012). It is regarded as the only commercial solution for substantial reduction of CO_2 emissions from power generation, iron and steel manufacturing, cement production, and chemical and processing industries.

In CCS, CO_2 is separated from other gases by post-combustion, pre-combustion, and oxy-fuel combustion techniques. Once CO_2 is separated, it is compressed and transported in a dense phase by pipelines, ships, and trucks, to injection sites. Where CO_2 is injected in the deep geological structures for storage or enhanced oil recovery and it is regarded as the final stage of CCS.

The CCS or sequestration of CO_2 in subsurface geological structures can play a key role to control CO_2 emissions (IPCC, 2005). Especially, depleted hydrocarbon reservoirs are important, because these reservoirs are studied in detail. They are monitored for long during hydrocarbon production, and also incremental oil and gas can be produced from these reservoirs by storing CO_2, thus giving economic benefits (Khurshid et al., 2014a).

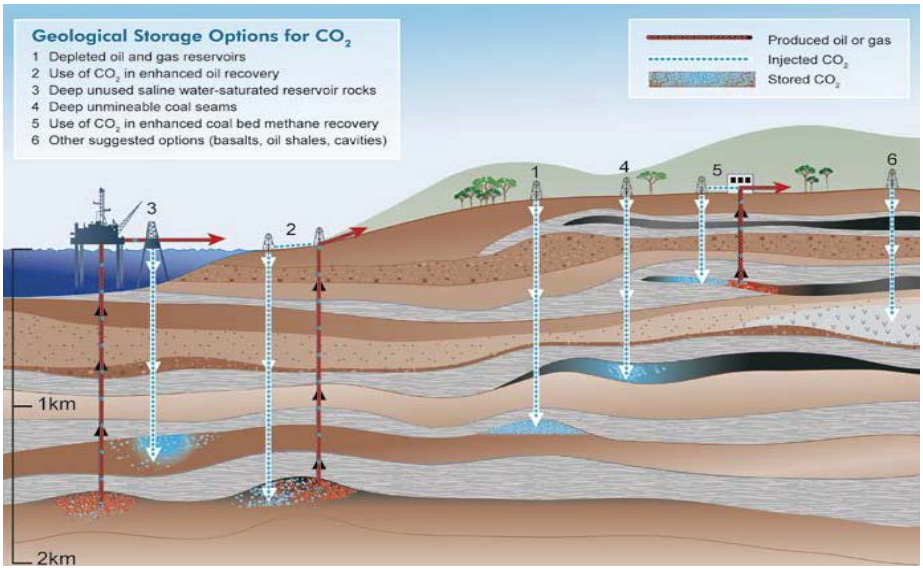

Fig. 1.1 Options for CO_2 geologic storage (IPCC, 2005).

1.2 Overview of CO_2 Enhanced Oil Recovery

Whenever a hydrocarbon reservoir is discovered and oil is produced, there are three phases in the production life of the reservoir: primary, secondary, and tertiary. We can typically produce 10-25% of the oil in place by the primary recovery, which includes natural drive

mechanisms: solution gas, gas cap drive, water influx, gravity drainage, or by their combination.

In the secondary recovery we may get additional 15-35% oil, by maintaining the reservoir pressure with water injection. However, 35-55% oil is still left behind in the reservoirs. This residual oil can be produced by enhanced oil recovery (EOR) methods. These methods include thermal, chemical, and solvent injection (Lake, 1989). Using CO_2 solvent flooding for EOR (CO_2 EOR) has proven successful in rejuvenating oil production from many depleted and matured oil fields.

CO_2 EOR is regarded as one of the most successful EOR method. Currently 130 CO_2 EOR projects are in operation globally and are producing 300,000 bbl of oil per day. The CO_2 price for EOR is 10-40 USD/ton (Godec, 2011). Roughly it requires 0.5 tonnes of CO_2/barrel of oil (Bloomberg, 2012).

The CO_2 produced by burning fossil fuels or other industrial processes is considered anthropogenic CO_2. This CO_2 is more expensive than naturally accumulated or geologic CO_2, because it requires physical and chemical process for separation. However, the use of anthropogenic CO_2 in CO_2 EOR is recognized as becoming economically viable because governments give tax incentives to mitigate carbon emissions, and also operators are interested in CO_2 EOR as geologic CO_2 sources are not always accessible. Therefore, CO_2 injection is being considered as a likely mean to advance the deployment of CCS technology globally.

1.3 Mechanism of CO_2 Enhanced Oil Recovery

The target of CO_2 EOR is reservoirs that lie at the depth greater than 800m, because the pressure and temperature at these depths maintain CO_2 at a supercritical state (IPCC, 2005). This phase has benefits of efficient oil recovery and improved storages of CO_2. The recovery of oil and its displacement by CO_2 strongly depend on reservoir permeability, porosity, thickness, pressure, depth, temperature, and oil compositions (Dai et al., 2013). There are two main type of CO_2 EOR: immiscible and miscible.

Immiscible CO_2 EOR is a process of CO_2 injection in which CO_2 and oil don't mix with each other due to low pressure and oil compositions. In this process the injected CO_2 saturates with the oil, swells it, reduces its viscosity and density, and extracts the light portion of the oil.

In miscible CO_2 EOR, the injected CO_2 develops multi-miscibility contact with the reservoir oil, when injected at a pressure of 100-300 bar (1450-4350 psi) depending upon reservoir temperature, pressure, oil compositions, and injected CO_2 compositions. However, if injected pressure of CO_2 is below minimum miscibility pressure (MMP), CO_2 can be injected, but the efficiency of the recovery process is adversely impacted.

The objective of miscible CO_2 EOR is to mix CO_2 with oil and form a single phase to reduce the oil saturation at the lowest level and to mobilize the oil stuck in the pores (Lake, 1989). The common practices during CO_2 EOR are: at wellhead CO_2 is supplied by a pipeline in high purity (>95% by volume), in a supercritical dense

phase pressure = 1400 psi, temperature = 23.88 ^{o}C, density = 53 lb/ft^{3} (Meyer, 2007).

Fig. 1.2 shows a schematic for CO_2 EOR. During this process, high pressure CO_2 first vaporizes the light component of the oil and then it condenses into oil phase in the reservoir, forming a single phase of CO_2 and oil. This single phase has low viscosity, enhanced mobility, and low surface tension. This is why miscible flooding results in high oil recovery.

However, CO_2 EOR has problems of mobility control, early breakthrough, and recycling. These problems can be managed by water-alternative gas (WAG), simultaneous water-alternative gas (SWAG), or foam assisted water-alternative gas (FAWAG) injection techniques.

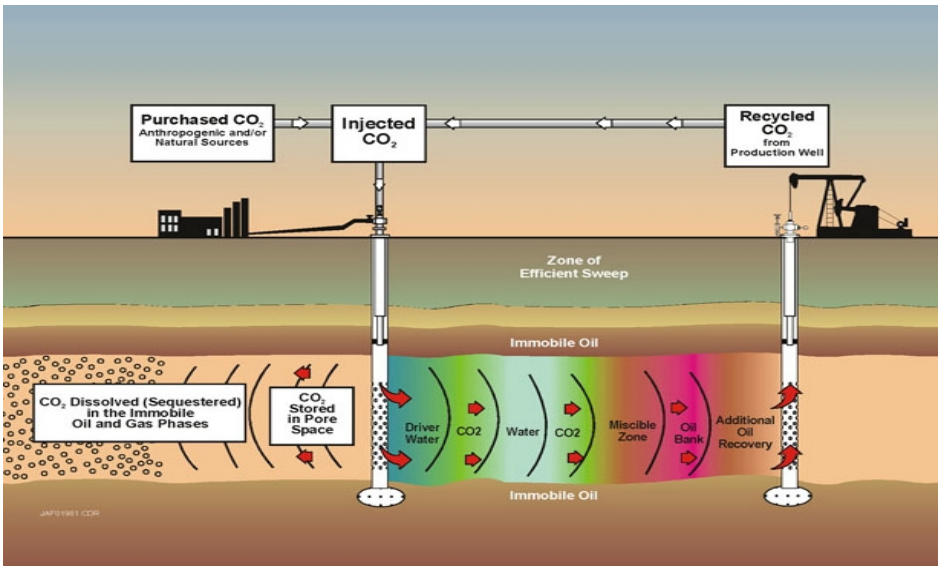

Fig. 1.2 Schematic for CO_2 EOR (Lake, 1989).

1.4 Review of Current CO_2 Enhanced Oil Recovery

Segall (1989) mentions that when pore pressure decreases with fluid extractions, it causes compaction of reservoir rocks and deforms the surrounding rock mass. Therefore, oil production results in increase of the effective stresses leading to pore collapse, surface subsidence and seafloor deformation (Jaeger et al., 2007; Zoback, 2007). Accordingly, it is important to know the time, pressure, and level of stresses that will lead to irreversible pore collapse and deformation.

Mohr's circle with pore pressure and stress coupling is commonly used to predict rock behavior in different stress regimes. However, it is based on the assumption that pore pressure has no effect on vertical stresses. Though, the change in pore pressure affects the entire stress tensor (Schutjens et al., 2012). At the same time the use of poroelastic equations for reservoir compaction is alluded because they are derived for homogenous, isotropic, linear poroelastic formation (Zoback, 2007). An additional reason for questioning the applicability of these equations is the assumption of no horizontal strain (Teufel et al., 1991). Therefore, there is need of a reservoir compaction prediction model to determine minimum reservoir pressure and an optimal time range to arrest pressure depletion, irreversible reservoir compaction, and to increase oil recovery and CO_2 storage.

When CO_2 is injected into a wellbore for EOR or sequestraion, the CO_2 may get heated with the geothermal gradient. The effect of temperature is usually neglected. However, the temperature of CO_2 is not typically same as geothermal gradient. It is a function of injection

rate, injection time, geothermal gradient, and surface temperature. The thermal impacts and chemical reactivity of CO_2 have been studied by many researchers (Gaus et al., 2008; André et al., 2009; Matter and Kelemen, 2009; Xiao et al., 2009). They mentioned CO_2 temperature is key factor in its hydrodynamic trapping, dissolution, and mineral trapping. Moreover, accurate temperature of CO_2 is important because it governs both the fluid state (liquid, gaseous, or supercritical CO_2) and the chemical reactivity.

There have been lots of studies for temperature prediction for drilling mud and other fluids (Ramey, 1962; Arnold, 1990; Romero and Touboul, 1998; Hasan and Kabir, 2002; Apak and Ozbayoglu,2009; Khurshid et al., 2013). However, they all assumed constant thermodynamic properties and ignored the change in fluid properties with pressure and temperature. Therefore, this phenomenon may cause imbalance of vapor/liquid equilibrium and will lead to erratic temperature prediction.

During primary production, reservoir depletion leads to phase separation and compositional change. This change may shift the reservoir equilibrium conditions. Furthermore, when CO_2 is injected for EOR activities it may change compositions and pH of oil, leading to deposition of asphaltenes (Gruesback and Collins, 1982; Srivastava et al., 1999; Civan, 2000; Wang and Civan, 2001; Mathiassen, 2003; Wan et al.2011; Zanganeh et al., 2012). The injected CO_2 may react with reservoir rock, leading to its dissolution and precipitation of carbonate particles (André et al., 2007; Gaus et al., 2008; Matter and Kelemen 2009; Zeidouni et al., 2009; Bacci et al. 2011, Wang et al., 2011). Their works either demonstrated asphaltene, or the dissolution

and precipitation of carbonate particles. They also overlooked the cementation of asphaltene and carbonate particles.

Regarding the optimization of CO_2 injection and EOR, there are two main approaches: production optimization and computational optimization. A lot of work is done on different methods of CO_2 injection to increase oil recovery (Mathiassen, 2003; Jessen et al., 2005; Kovscek and Cakici, 2005; Jahangiri and Zhang, 2011; Dai et al., 2013). At the same time much work is done on different techniques of computational optimization (Kolda et al., 2003; Echeverria et al., 2011; Cameron and Durlofsky, 2012) to find the optimize solution with low numeric effort. All of them researched either production or computational optimization. However, there is dire need of coupled optimization to increase oil recovery, CO_2 storage and at the same time decrease formation damages.

1.5 Research Objectives and Motivation

The target of this dissertation is to investigate different mechanisms and several aspects of CO_2 EOR to better understand and explore those factors that limit the performance of CO_2 EOR. The research also presents that if these factors are dealt as per recommendations of this study, it will enhance performances of CO_2 EOR activities.

The overall aim of this research is to come out with solutions and procedures by which operations and practices in the CO_2 EOR activities can be modified. This will help to increase oil recovery and

CO_2 storage, and decrease formation damages. The following are the main objectives of this study:

1. To develop a generic integrated framework for reservoir compaction to determine the minimum reservoir pressure after which permanent pore collapse will initiate. This approach helps to determine an optimal time range of CO_2 injection in a reservoir for increasing its storage and oil recovery.
2. To develop a simulator to predict accurate temperature of CO_2, thermal disturbances, control the dynamic behaviors of injected CO_2 in shallow and deep reservoirs.
3. To develop a comprehensive formation damage model that considers the fluid flow, chemical reactivity, particle transport, and particles deposition.
4. To develop an integrated methodology to optimize CO_2 storage and oil recovery by re-dissolving and removing the deposited asphaltene.

Key achievements of this research are based on analytical analyses, numerical investigations, modeling, and sensitivity analyses. For the successful development of models and simulators, it is important to consider many factors such as reservoir compaction, thermal modeling, formation damage, the deposition of asphaltene, source of chemical components that take part in the carbonate dissolution reaction, and cementation of carbonate particles and asphaltene, and the change in porosity due to their cementation.

1.6 Outline of the Dissertation

The thesis is composed of six chapters and its outline is as follows. Chapter 1 provides introduction and brief information on the need of CCS and CO_2 EOR including the objectives and scopes of the dissertation.

Chapter 2 explains an analytical model developed to predict a critical point of pore collapse. This model along with the proposed failure-line methodology determines an optimal time range and minimum reservoir pressure after which, permanent pore collapse will occur. By using this minimum reservoir pressure we can make a proper schedule for CO_2 injection. This chapter also shows the verification of results with experimental and field data available.

Chapter 3 describes the development of a simulator by solving the equation of heat transfer for CO_2 and incorporating experimentally determined thermodynamic properties of CO_2. This chapter also presents detail analyses of different injection parameters that affect the temperature of CO_2.

In chapter 4, this study determines the amount of irreversible formation damages with CO_2 EOR. The developed formation damage model combines and forecasts the rate of asphaltene deposition, rock dissolution, and precipitation of the dissoluted particles. This chapter also presents searching of different injection parameters to control formation damages.

In chapter 5, detail simulation study is performed to develop an integrated methodology to minimize asphaltene deposition in

reservoir pores, and to increase oil recovery and CO_2 storage. The methodology consists of injection scenario for CO_2 based on sensitivity analysis to optimize oil recovery and CO_2 storage, and to reduce the amount of deposited asphaltene by its redissolution and removal. This chapter also shows the analyses of different heterogeneities and fluid compositions to determine their effects on asphaltene deposition.

Chapter 6 provides the conclusions and the future perspectives on CO_2 EOR based on the outcome of this study. This chapter also highlights the most significant results listed in chapters 2 to 5 and relates the findings to the current state of the art.

Chapter 2

ANALYTICAL MODEL TO DETERMINE MINIMUM RESERVOIR PRESSURE AND OPTIMAL TIME RANGES FOR CO_2 INJECTION IN A RESERVOIR

2.1 Reservoir Compaction

Oil and gas reservoirs are natural containers buried in the deep earth containing different reservoir fluids. At a certain depth, net effective stresses are equal to the overburden stresses minus the pore pressure. The overburden compacts the rock. However, the pore pressure resists the compaction and pore space reduction.

Reservoir pressure decreases when oil/gas is produced. Consequently, it leads to pore collapse and compaction (Aadnoy, 1991). Its magnitude depends on the amount of production, mobility, solubility, density, and compressibility of various pore fluids and rock, and also on the reservoir boundary conditions: faults, edge or bottom water (Geertsma, 1973).

When the pore pressure decreases with fluid extractions, it causes compaction of reservoir rocks and deforms the surrounding rock mass (Segall, 1989). The Ekofisk field had an initial pore pressure of 45 MPa, but it was subsequently reduced to 20 MPa with production. This reduction caused reservoir compaction and the platform air-gap reduced to approximately 10 ft (Addis, 1997).

The pore pressure decrease causes an increase in the effective stresses on rock skeleton and triggers reservoir deformation in three distinct mechanisms: reservoir compaction, poroelastic behavior, and faulting (Teufel et al., 1991). Zhu and Wong (1997) conducted triaxial compression experiments and observed that the stress increase causes a consistent decrease in permeability and the strain increases independent of, whether it is strain softening or hardening, or by shear localization. Zhang et al. (1990) mentioned that porosity reduction evolves gradually as matrix material deforms and proceeds from elastic to elastic-plastic and ultimately to fully plastic.

Thus, when a reservoir reaches its plastic limit, irreversible reservoir compaction initiates. This reservoir compaction causes volume reduction, grain rotation and sliding, and increase in acoustic wave velocity (Khurshid et al., 2014a). The volumetric variations of reservoir pore space cause manifold reduction in permeability leading to loss of productivity. Davies and Davies (2001) mentioned that with depletion the most significant permeability loss occurs in rock with slot (long, narrow) pores, while pores with bundle of tubes are least affected.

2.2 Interaction of Pore Pressure and Stress

The effects of pore pressure, its reduction and increase can be explained by the theory of effective stresses that is explained by Terzaghi's law (Zoback, 2007).

$$P_{eff} = P_{ob} - \mu P_i \qquad (2.1)$$

Where, P_{eff} is the effective pressure in psi. P_{ob} is the overburden pressure in psi, μ is ratio of poroelasticity, and P_i is the initial pore pressure in psi. The pore pressure counteracts the overburden stresses, as fluid is not able to take or transfer any shear stresses. Thus, it affects the principal effective stresses while no affect on shear stresses. The affects of effective state of stress can be explained by Mohr's circle.

There are two cases, one in which pore pressure decreases (production) and other where the pore pressure increases (injection). If it is assumed that the total stresses are independent of pore pressure. Then for both of these cases, the differential stresses (the difference of maximum and minimum principal stresss) are constant. While the effective stresses (mean of maximum and minimum principal stresses) changes by the amount of change in pore pressure.

From Fig. 2.1 it can be observed that, the pore pressure has no effect on the shear stresses. The Mohr's circle doesn't change in the diameter because the differential stresses remain constant and there is only a horizontal shift. However, field observations of production have shown that the change in pore pressure is dependent or coupled with total stresses (minimum and maximum horizontal stresses). To know the effect of this couple affect it is important to consider different stress regimes such as normal, thrust and reverse to predict rock stability.

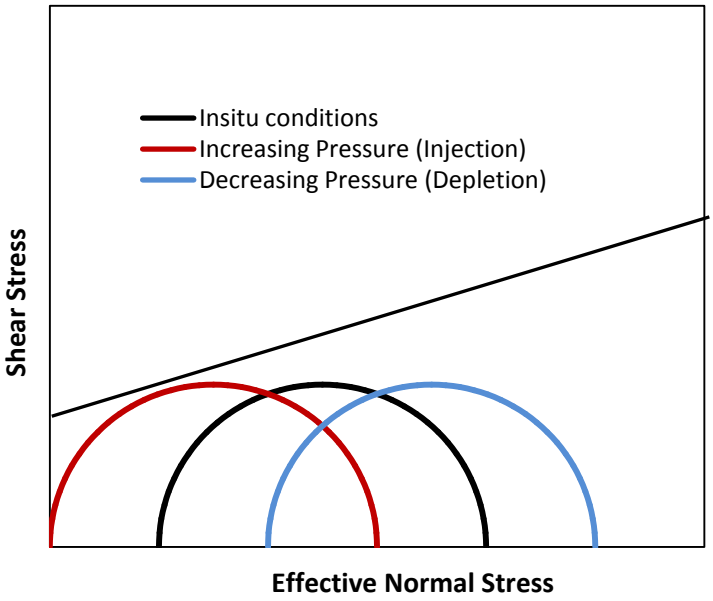

Fig. 2.1 Mohr's circle at assuming total stresses independent of pore pressure.

In normal stress regime we have $\sigma_v > \sigma_H > \sigma_h$, where σ_v is the maximum and σ_h is the minimum stress. From Fig. 2.2 it can be observed that in normal stress regime, injection will lead to smaller Mohr's circle while production to larger Mohr's circle. With production the size of the circle increases accompanied by decrease in pore pressure, as effective horizontal stresses increases but the total horizontal stresses decreases with the decrease in pore pressure. This leads to an increase in the effective vertical stresses and size of the circle.

However, for injection case the diameter of the circle reduces because the effective horizontal stresses decreases with the increase

of pore pressure (Hillis, 2000). This reduction of differential stresses with pore pressure increase may lead to stabilization in normal stress regime.

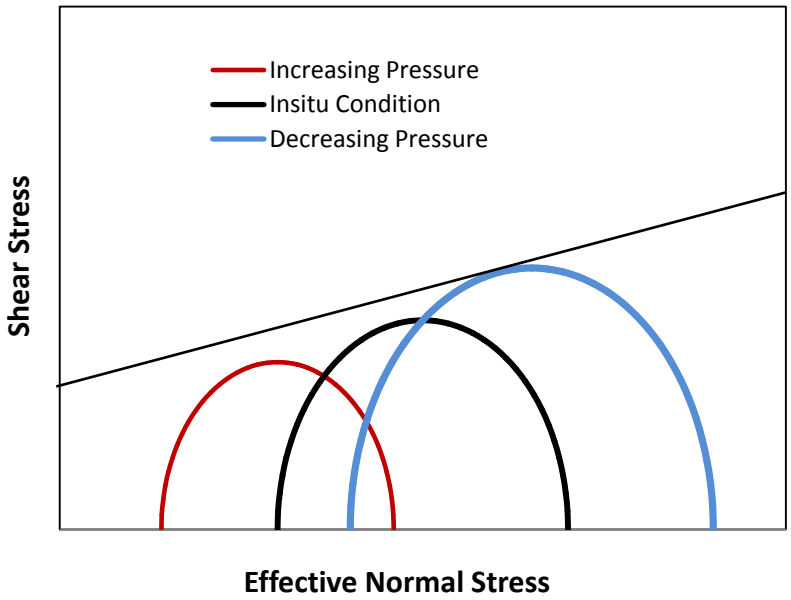

Fig. 2.2 Mohr's circle for normal stress regime.

For thrust stress regime we have $\sigma_H > \sigma_h > \sigma_v$, where σ_H is the maximum and σ_v is the minimum stress. This phenomenon causes an opposite effect as normal stress regime. It can be observed from Fig. 2.3 that in thrust stress regime, injection will lead to large Mohr's circle while production to small Mohr's circle.

With injection the increase in pore pressure causes an increase in differential stresses and vice versa. It can be observed that, in this regime production leads to stabilization as the pore pressure reduction leads to low differential stresses.

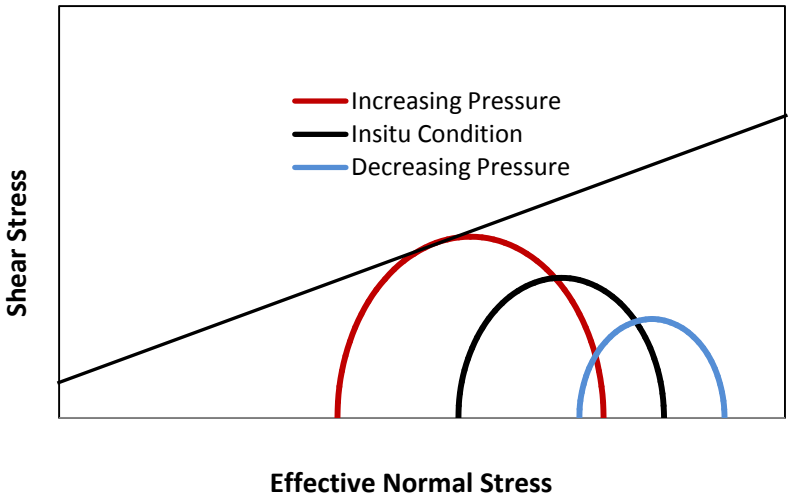

Fig. 2.3 Mohr's circle for thrust stress regime.

In a strike-slip regime we have $\sigma_H > \sigma_v > \sigma_h$, where σ_H is the maximum and σ_h is the minimum stress. Therefore, the change in pore pressure doesn't affect the differential stresses and size of the Mohr's circle. The circle only shift horizontally during injection and production as shown in Fig. 2.1. It can also be observed that production leads to more stable state of stress while injection is causing more instability.

To determine the effect of reservoir compaction a lot of models have been developed to estimate the stress path. The elastic uniaxial strain model in Eq. (2.2) predicts initial horizontal stresses and production-induced changes by these stresses. It predicts total horizontal stresses from the calculations of overburden stresses, pore pressure, and Poisson's ratio.

$$S_H = \left(\frac{\nu}{1-\nu}\right)\left(S_v - \mu P\right) + \mu P \qquad (2.2)$$

Where, S_H is the horizontal stress in psi, S_v is the overburden stress in psi, ν is the Poisson's ratio, and μ is the poroelastic parameter. In terms of effective stress the above equation can be written as

$$\sigma_H = \left(\frac{\nu}{1-\nu}\right)\sigma_v \qquad (2.3)$$

Where, σ_H and σ_v are the effective horizontal and vertical stresses, respectively. In the above model horizontal stresses increases with depth, and with pore pressure or change in lithology (i.e. the Poisson's ratio).

The use of poroelastic equations (2.1-2.3) for reservoir compaction is alluded because they are derived for homogenous, isotropic, linear poroelastic formation (Zoback, 2007). Another reason for questioning the applicability of these equations is the assumption of no horizontal strain (Teufel et al., 1991). At the same time the use of Mohr' circle with pore pressure and stress coupling is based on the assumption that pore pressure has no effect on σ_v. However, it is found that the change in pore pressure affects the entire stress tensor (Schutjens et al., 2012). Therefore, using these approaches results in erratic reservoir compaction prediction behavior. Therefore, there is need of a reservoir compaction prediction model to determine minimum reservoir pressure and an optimal time range to arrest pressure depletion, irreversible reservoir compaction and to increase oil recovery and CO_2 storage (Khurshid et al., 2014a).

2.3 Effects of Reservoir Compaction

Reservoir compaction may also act as a drive mechanism providing energy for production up to 45-75% of total energy and can increase the recovery (Settari, 2002). However, it causes severe environmental problems such as surface subsidence, and seafloor deformation, sinking of offshore platforms, buckled seabed pipelines, and operational problems.

It may change fracturing strength of the formation leading to well failures such as casing and liners collapses. It can induce reactivation of faults, deformation of overlying formations, and affects the integrity of the cap rock. Other potential problems are: it may constraint the infill drilling plan, and hydraulic fracturing design. From the reserve estimation point of view, reservoir compaction may result in under or over estimation of reserves due to inaccurate estimation of compressibility factor (Khurshid et al., 2014a).

Therefore, an analytical model is developed by using the concept of pore arrangement at macroscopic scale. This model along with the proposed failure-line methodology determines a minimum reservoir pressure after which permanent pore collapse will occur. By using this minimum reservoir pressure, we determine an optimal time range for CO_2 injection. This concept is not utilized before to characterize irreversible formation damages and reservoir compaction phenomenon. Fig. 2.4 demonstrates flowchart for the determination of minimum reservoir pressure.

The results of the developed model and the methodology are also verified with experimental and field data available, giving a good match. The developed model and methodology provides useful insights to understand the reservoir compaction and dynamic behavior of stresses in a reservoir, and to control reservoir compaction.

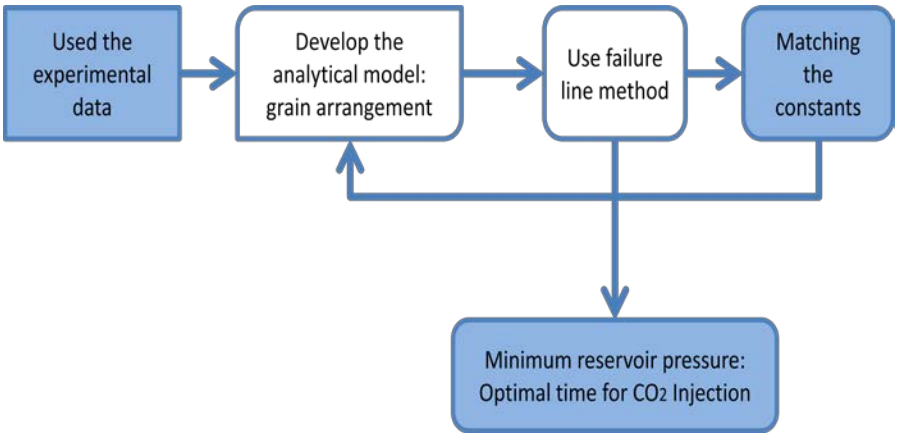

Fig. 2.4 Flowchart for the determination of minimum reservoir pressure.

2.4 Reservoir Compaction Prediction Model

A reservoir rock is an aggregate of minerals with pores saturated with fluids such as water, oil, or gas. These fluids and their pressures have important affect on the mechanical behavior of the rock. When reservoir pressure and its pore fluid decreases, it initiates deformation in the form of reservoir compaction. This compaction depends on the rate at which overburden load is applied.

When the applied load is immediate, the pore pressure increases. However, when the applied load is low and continuous, the pore pressure decreases because enough time is available to drain away the fluids. This fluid withdrawal leads to the compaction or pore collapse. Therefore, a model is needed to predict the minimum reservoir pressure, rock compaction, its behavior, effect, and an optimal time range to control it (Khurshid et al., 2014a). The model description is as follow.

Consider a rock at macroscopic scale in which the pores are arranged in a body-centered cubic lattice as shown in Fig. 2.5. The Pythagorean Theorem suggests that the square of the diagonal across the body of a cube is the sum of the squares of three sides. By taking the square root and subtracting the radius, the distance between pores is derived, which is given by

$$d = \frac{\sqrt{3}}{2}a - 2r \qquad (2.4)$$

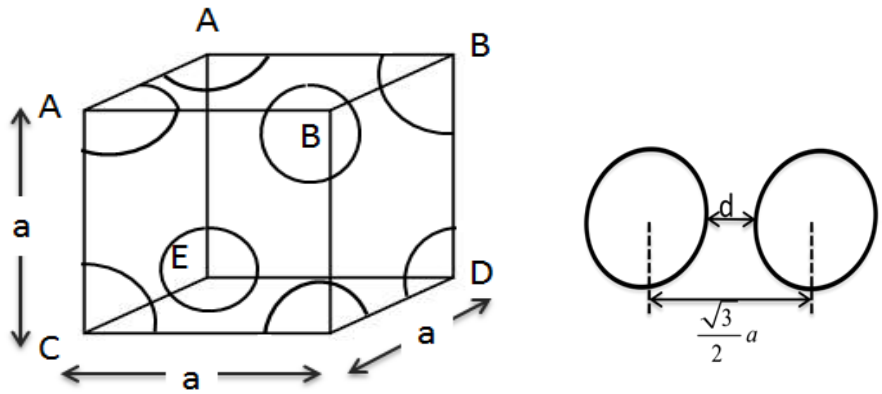

Fig. 2.5 Body-centered pores in a cubic lattice at macroscopic level.

Where, *r* is the radius of the pores, *d* is the shortest distance between pores, and *a* is the unit lattice edge length.

Thus, for two pores in an unit lattice the following equation is used for porosity ϕ, and it is given by

$$\phi = \frac{8\pi r^3}{3a^3} \tag{2.5}$$

From Eq. (2.5) we get the radius

$$r = \left(\frac{3a^3\phi}{8\pi} \right)^{1/3} \tag{2.6}$$

In equation (2.4) putting the value of pore radius, the distance between the pores is obtained

$$d = \frac{\sqrt{3}}{2}a - 2\left(\frac{3a^3\phi}{8\pi} \right)^{1/3} \tag{2.7}$$

Considering the stress in the rock matrix, where the stresses are dependent on square of distance between the pores and the length of unit lattice.

$$\sigma \propto \frac{1}{\left(\frac{d}{a} \right)^2}$$

The effective stresses σ, due to the axial stress σ_a is given as

$$\sigma = \frac{\sigma_a}{A(d/a)^2} \tag{2.8}$$

Where A is the constant. Assuming that the pore collapse occurs when $\sigma = \sigma_c$

$$\sigma_a = A\sigma_c (d/a)^2 \qquad (2.9)$$

Putting the value of the distance between pores from Eq. (2.7) into Eq. (2.9)

$$\sigma_a = \beta\left\{\frac{\sqrt{3}}{2} - 2\left(\frac{3\phi}{8\pi}\right)^{1/3}\right\}^2 \qquad (2.10)$$

Where, $\beta = A\sigma_c$. Generalizing Eq. (2.10), which is only for the body central cubic lattice, the following equation is proposed.

$$\sigma_a = \beta(\alpha - \gamma\ \phi^{1/3})^2 + \delta \qquad (2.11)$$

Where, α is the constant showing the central distance between the pores, and γ is the constant depending on geometry and layout of pores. δ is used because actual rock has some strength at $\phi(\sigma_{min})$ as shown in Fig. 2.6.

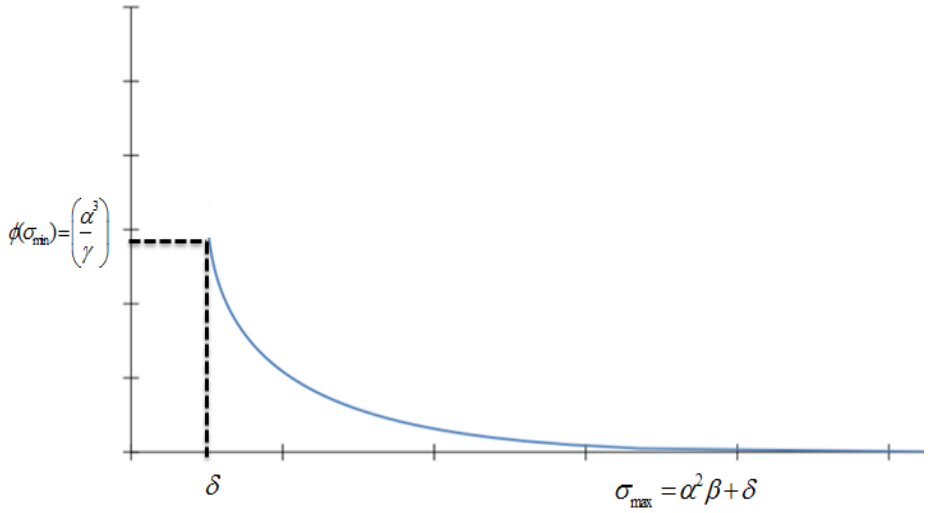

Fig. 2.6 Behaviors of porosity and pore collapse stress at different stress levels.

2.5 Results and Discussions

The reservoir compaction can be controlled by pressure maintenance such as hydrocarbon gas injection, waterflooding, or CO_2 injection. CO_2 injection has a couple of benefits: it can control pressure drop, arrest reservoir compaction, reduce CO_2 emissions, and also result in extra oil recovery.

Moreover, hydrocarbon reservoirs are studied and monitored for long time, they are best candidates to control CO_2 emissions and for its storage and sequestration (IPCC, 2005). Therefore, CO_2 injection is one of the best options to control reservoir compaction.

However, it is very important to inject CO_2 in a reservoir before pore collapse to have optimum oil recovery and CO_2 storage. Rutqvist et al. (2008) performed tensile and shear failure analyses for CO_2 injection pressure. They mentioned that to recover oil from compacted zone, if CO_2 injection pressure is raised above the initial reservoir pressure. This action may trigger shear failure along pre-existing fractures. This phenomenon may activate pre-existing fractures and develop new fractures/path-ways in the reservoir. Then the injected CO_2 will flow through these opened or new fractures, and the oil in the compacted zone cannot be recovered. Thus we will lose a portion of the reservoir for CO_2 storage and oil production.

To determine the values of constants in the developed analytical model in Eq. (2.11), the experimental data of rocks is utilized. However, the compaction behavior is a very complex phenomenon depending on grain size, shape, strength, and orientation. Therefore, experimental data at uniaxial strain conditions is employed to mimic the reservoir conditions where the radial stresses were maintained at zero lateral strain. Thus, data from Smits et al. (1988) are used to simulate field conditions as closely as possible.

Fig. 2.7 demonstrates an average trend of the experimental data from Smits et al. (1988). By performing trial and error method the parameters in the developed model are determined.

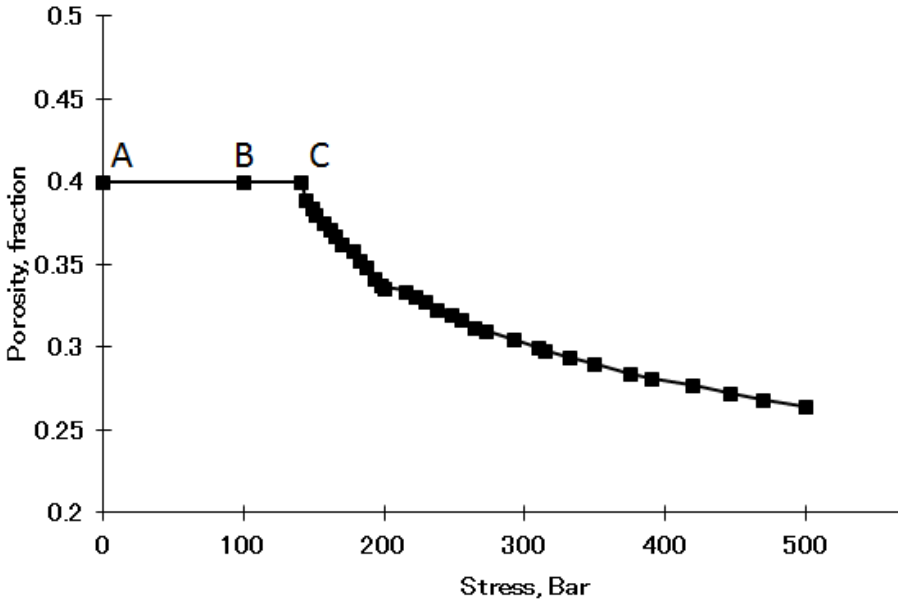

Fig. 2.7 Plot of average values of stresses versus porosity at different initial porosity (data from Smits et al. 1988).

In Fig. 2.7, point A shows an imaginary porosity at the atmospheric pressure. The pore pressure decreases from point B somewhere on the line by production. It can be observed that the porosity of the rock remains relatively constant. However, when point C is crossed, porosity decreases exponentially due to the increase of the effective stresses. The linear trend in Fig. 2.7 from point A to C shows the elastic limit. However, when the load exceeds this limit (point C) reservoir compaction starts and then increases at a high rate.

In this study, the point C is called as the starting point of the failure-line. Once this point of the failure-line is crossed, the porosity of the rock decreases exponentially with stresses. Therefore, to store CO_2 and to recover maximum oil from the reservoir, it is suggested to

inject CO_2 between point A to B, this presents the optimal CO_2 injection time range. However, injecting CO_2 after point C will result in decreased storage and reduced oil recovery due to pore collapse.

To find the parameters in Eq. (2.11), a detailed sensitivity analysis is performed to match the results of the developed model with averaged experimental data from Smits et al. (1988). From the results in Fig. 2.8, different matches of the developed model can be observed with the averaged experimental data. An excellent match is achieved for the value at α = 1.33, β = 1980 psi, γ = 0.984, and δ =100 psi in Fig. 2.8(b).

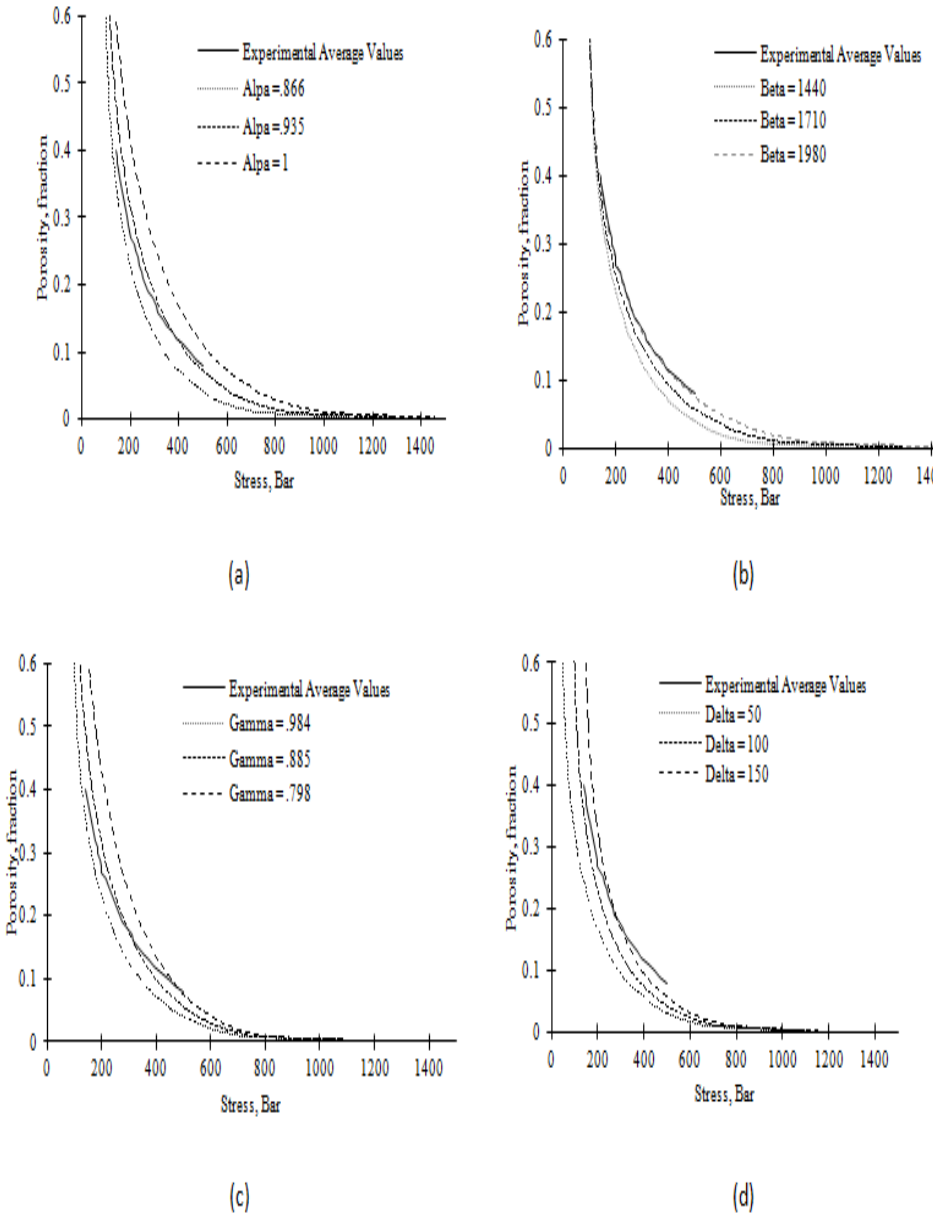

Fig 2.8. Matching of the model parameters with experimental average values (a) Varying values of Alpha with constant β=1440, γ=.984 and δ=50 values (b) Varying values of Beta with constant α=.866, γ=.984 and δ=50 values (c) Varying values of Gamma with constant α=.866, β=1440 and δ=50 values (d) Varying values of Delta constant α=.866, β=1440, and γ=.984 values.

2.6 Methodology for Field Applications

The failure-line technique introduced in this study can be easily used to determine minimum reservoir pressure and an optimal time range for CO_2 injection in a reservoir, for maximum CO_2 storage and oil recovery. The procedure for the failure-line methodology is as follow.

1. For a reservoir rock (by coring), a trend can be established by performing a series of uniaxial compaction test with a range of initial porosities.
2. After compaction tests, determine porosities and plot them. A trend of porosity with pressure will be obtained.
3. Then match the experimental data with the analytical model proposed.
4. From the match, determine the values of α, β, γ, and δ.
5. Then draw a horizontal line from the initial porosity towards the plot. When the drawn line intersects the curve, it gives the value of stress that will cause the pores to collapse. The line will be inclined if the elastic deformation is considered. However, ignoring this elastic deformation will produce small stress, which results in safer side solution.
6. The analysis is a procedure for a single layer reservoir. However, for a multilayer reservoir it is advisable to perform the procedure mentioned above for each layer.
7. Therefore, the interval before the point of failure shows minimum reservoir pressure and an optimal time range for CO_2 injection as shown in Fig. 2.9.

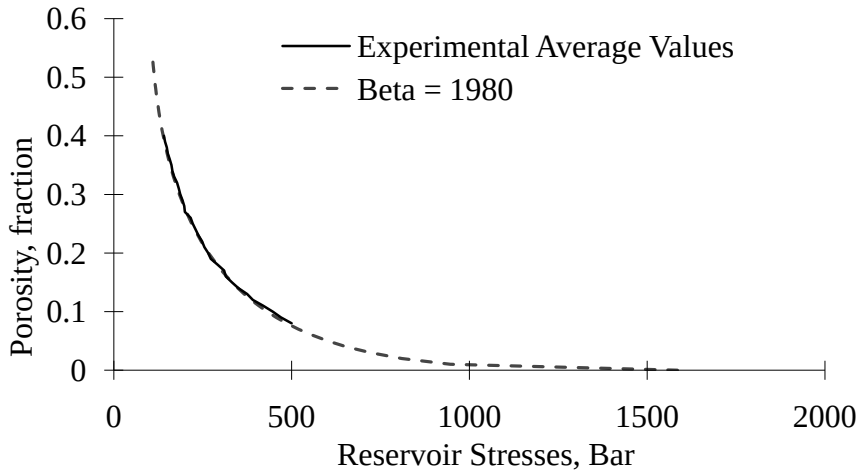

Fig. 2.9 Matching of experimental data with the analytical solution.

2.7 Validation and Case Study

The data from the Valhall field, North Sea is used to prove the importance and efficiency of the developed model and methodology. Since, this field has compaction drive mechanism for its production, the earthquake or seismicity is not caused due to production (Corzo et al., 2013). Also the field has high to low porosity ranges and was extremely over-pressured at reservoir pressure of 6555 psi (45.2 MPa). Therefore, these extreme complexities and uncertainties in the reservoir properties can perfectly identify the effectiveness of the model.

Fig. 2.10 shows the results of the developed methodology using the failure-line technique. A good match can be observed between the predicted compaction and pore collapse with actual field data from Corzo et al. (2013). Their data is based on geomechanical

model calibrated using core data, seafloor subsidence records, gravimetric data and radioactive bullet markers. As can be seen in Fig. 2.10, their data are well matched by the model proposed. The parameters determined for Valhall field are: (1) 32% porosity: α = 1.167, β = 8375, γ = 0.984, and δ = 500 psi and (2) 42% porosity: α = 1.33, β = 16750, γ =1.0838, and δ = 100 psi.

From Figs. 2.10 (a) and (b), it can be observed that the irreversible reservoir compaction occurs, when pore pressure reached 2500 and 5000 psi with initial porosity 32% and 42%, respectively. It is evident that, both curves intersect the failure curve and prove the validity of our model. However, the data cut the line of failure at different stress levels because of different initial reservoir porosity. This implies that, reservoir compaction is dependent on initial reservoir porosity and rock strength.

It is found that when reservoir pressure decreases, the stresses in the reservoir increases to a critical level leading to irreversible deformation and pore collapse. This finding shows that if the pressure of the Valhall field would have been maintained before reaching 5000 psi, reservoir compaction would have controlled. As a result, more oil would have been recovered. So, the application and the results prove the applicability and benefits of the developed methodology.

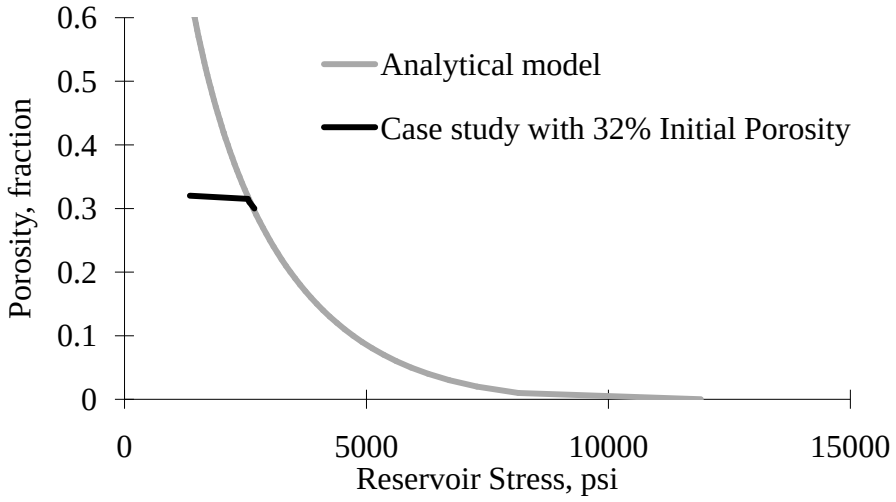

(a) 32% porosity

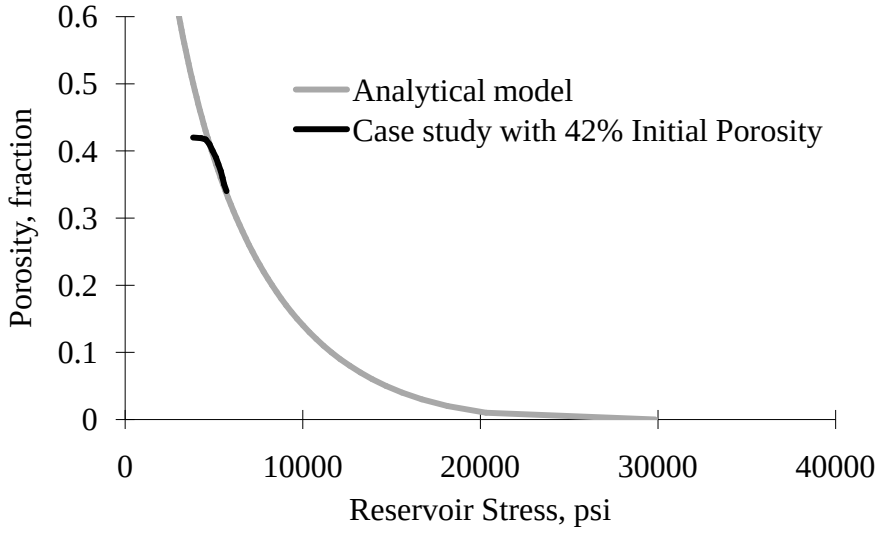

(b) 42% porosity

Fig. 2.10 Validation and comparison of the developed model with field data of Valhall field, North Sea (data from Corzo et al., 2013).

2.8 Summary

1. In this study an analytical model is derived to predict reservoir compaction by considering the arrangement of pores at macroscopic scale in a reservoir rock.
2. On the basis of the model a failure line methodology is developed to determine minimum reservoir pressure and an optimal time ranges for CO_2 injection. Thus, it is suggested to inject CO_2 in a reservoir before touching the failure line, which can easily be determined to enhance CO_2 storage and oil recovery.
3. The developed model and the failure-line methodology can be used to investigate and predict the effect of pressure depletion, reservoir compaction, to determine the critical pore collapse stress point, and an optimal time ranges for CO_2 injection.
4. The proposed model and methodology is validated with experimental as well as field data available. The good agreement between the predicted pore collapse behavior and the field data proves the accuracy of our work.
5. Further, this study has revealed key insights into the reservoir compaction, and it depends on the pressure, production rate, porosity, geometry of the pores. Understanding these factors will be critical in terms of determining the dynamic geomechanical behavior of the reservoir rock easily and cost effectively.

Chapter 3

THERMAL MODELING OF CARBON DIOXIDE DURING ITS INJECTION IN SHALLOW AND DEEP RESERVOIRS

3.1 Thermal Modeling

Geological sequestration of CO_2 offers a possible, reliable, and promising solution for the reduction of CO_2 emissions. It has a potential to reduce CO_2 emissions at a low mitigation costs (IPCC, 2005). The sequestration of CO_2 in oil and gas reservoirs, coal seams, organic rich shale formations, and saline aquifers are gaining interest because they can be some of the best and safe natural containers. These containers are able to store CO_2 efficiently and safely for long periods of time (White et al., 2005). However, for these operations it is important to know physical, chemical, and thermal disturbances caused by CO_2 injection (Khurshid and Choe 2014b).

When carbon dioxide is injected into a reservoir, it dissolves into the water and increases the acidity of the formation water. Gaus et al. (2008) performed geochemical and solute transport modeling of CO_2 and found that CO_2 injection may acidize the media causing carbonate dissolution, leading to porosity increase. It is mentioned by Matter and Kelemen (2009) that the solubility of CO_2 decreases with increasing temperature and water ionic strength. Xiao et al. (2009) revealed that CO_2 solubility needs special modeling and it depends on

temperature, pressure, and formation properties. The thermal impact of CO_2 and its chemical reactivity on a carbonate saline aquifer were analyzed by André et al. (2009). They found that CO_2 hydrodynamic trapping, dissolution, and mineral trapping are highly sensitive to the temperature of CO_2 and affect its sequestration. Thus, it is essential to predict CO_2 temperature accurately when it enters into a reservoir or aquifer.

The effect of temperature is usually neglected. However, the temperature of CO_2 is not typically same as geothermal gradient. It is a function of injection rate, injection time, geothermal gradient, and surface temperature (Khurshid and Choe, 2014b). Moreover, accurate temperature of CO_2 is important because it governs both the fluid state (liquid, gaseous or supercritical CO_2) and the chemical reactivity. It is a complex problem to predict CO_2 temperature during its injection as it may exist in multiphase as shown in Fig. 3.1.

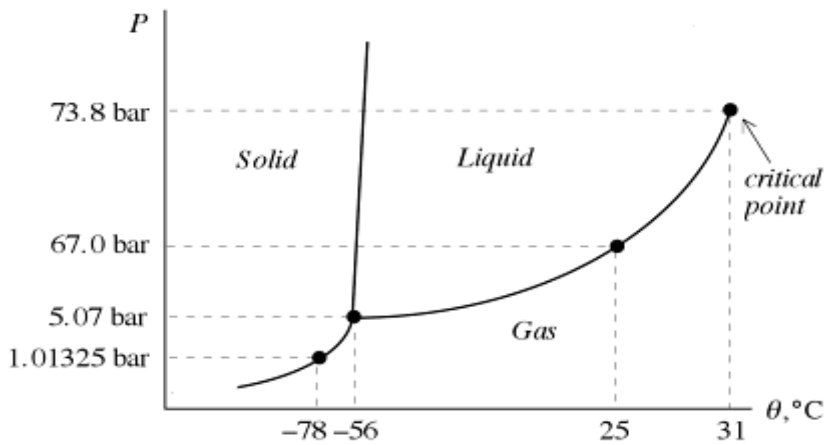

Fig. 3.1 Pressure-Temperature phase diagram for CO_2 (Foulkes, 2013).

Ramey (1962) and Arnold (1990) studied thermal behaviors of drilling fluids in a wellbore using heat transfer governing equations. Apak and Ozbayoglu (2009) employed finite element method to calculate the distribution of heat in a wellbore. Khurshid et al. (2010) analyzed the heat transfer and wellbore stability analysis in gas hydrate bearing formation in East Sea South Korea. Khurshid et al. (2013) developed a thermal simulator for predicting wellbore temperature distributions in deep wells and also examined thermal disturbances caused due to the flow of the heated mud. However, there is a need of an analytical model to predict the CO_2 temperature, analyzed the factors and formation damages caused due to heated CO_2 (Khurshid and Choe, 2014b).

The focus in this chapter is to present the development of a simulator that considers the change in CO_2 thermodynamic properties with the change in temperature. If one ignores the change of CO_2 properties, it will cause imbalance of CO_2 vapor/liquid equilibrium that may lead to erratic temperature prediction. Thus a simulator is developed by solving the equation of heat transfer for CO_2 injection and incorporating experimentally determined thermodynamic properties of CO_2 by Wark Jr. and Richards (1999).

The results of the developed simulator are validated with field and experimental data. The effects of heat transfer and formation damage with CO_2 Injection are also determined. Therefore, the proposed approach of using the experimental determined specific heat values of CO_2 gives accurate temperature prediction for injected CO_2. Sensitivity analyses of different injection parameters is also performed and it is found that the geothermal gradient, injection rate,

injection time, and surface temperature play a key role in controlling CO_2 temperature in sequestration activities.

3.2 Development of CO_2 Thermal Model

The common practices during CO_2-EOR are, at wellhead CO_2 is supplied by pipeline in high purity (>95% by volume), in a supercritical dense phase pressure=1400 psi, temperature =23.88 ^oC, density= 53 lb/ft^3 (Meyer, 2007). At these conditions during CO_2 injection, heat flows from the surrounding formations to the wellbore and subsequently to the CO_2 inside the tubing. During drilling and well completion for CO_2 injection, it is important to know the wellbore temperature profile. The estimation and prediction of CO_2 temperature profile will help to select the proper 1) Cement, its composition, placement and setting time 2) Corrosion in casings and tubings 3) Thermal stresses in casings and tubings 4) Packer design and selection 5) Logging tool design 6) Wellhead and production equipment design, etc.

The simulator developed can be used to model and determine the thermal disturbance in shallow and deep formations due to the heated CO_2. Fig. 3.2 shows the flowchart of the methodology employed in this study to predict CO_2 thermal behaviors.

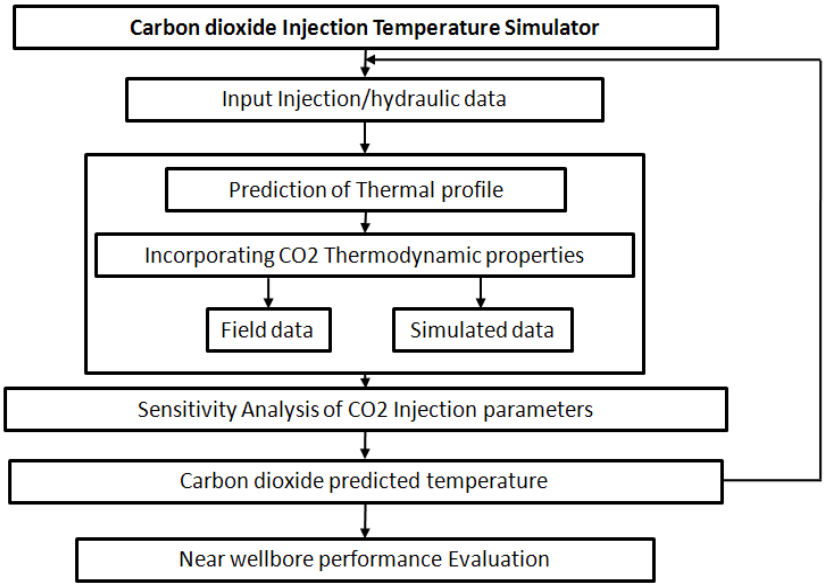

Fig. 3.2 Flowchart for the prediction of carbon dioxide (CO_2) behaviors.

The temperature in the surrounding rock is determined by the following equation.

$$\frac{\partial^2 T_f}{\partial r^2} + \frac{1}{r}\frac{\partial T_f}{\partial r} - \frac{c_f \rho_f}{k_f}\frac{\partial T_f}{\partial t} = 0 \qquad (3.1)$$

Where, T_f is the formation temperature in °C at an arbitrary depth at time t, r is the distance measured from the centre of the tubing in m, and c_f, ρ_f, and k_f are the heat capacity in KJ/kg-°C, density in kg/m^3, and thermal conductivity of the formation in KJ/hr-m-°C, respectively.

3.3 Heat Transfer from Formation to CO_2

When CO_2 is injected in the tubing, CO_2 gains heat from the formation through the section of casing and cement of the wellbore. The thermal behavior of CO_2 in tubing has the following stages. In the first stage, carbon dioxide passes through the wellhead and enters into the tubing, and then reaches the target formation. While in the second stage, it is assumed that the CO_2 temperature at the exit of the tubing be same to the CO_2 temperature at the formation entrance. It is assumed that CO_2 reaches the reservoir in a vertical well with constant well parameters as shown in Table 3.1. The governing equation for the variation of CO_2 temperature with depth in the tubing is

$$m\frac{\partial T_c}{\partial Z}c_p + 2\pi r_t U_f (T_c - T_f) = 0 \qquad (3.2)$$

Where m is the injection rate in kg/hr, and C_p is the fluid specific heat in KJ/kg-°C. r_t is the tubing radius in m, U_f is the overall heat transfer coefficient between the tubing and the formation in KJ/hr-m^2-^{o}C, and T_c and T_f are the temperatures of the CO_2 and the formation in ^{o}C, respectively.

Fig. 3.3 shows a schematic of CO_2 injection in the wellbore and the associated heat transfer process over a differential element of length Δx. Fig. 3.3 also illustrates heat flow from the formation into the tubing section through convection (q_f). The rate of heat flow by convection into the tubing is much greater than the rate of heat conduction in the formation, because of low heat conductivity of the

formation. This fact is very important when modeling the heat transfer process in the wellbore.

The CO_2 in the tubing acquires heat from the formations via convection, and conduction through the tubing itself (q_t). There is heat flow in and out of the differential elements within the tubing due to the bulk flow of fluid. Where $q_{t(x)}$ and $q_{t(x+\Delta x)}$ are the heat flow in the tubing.

.

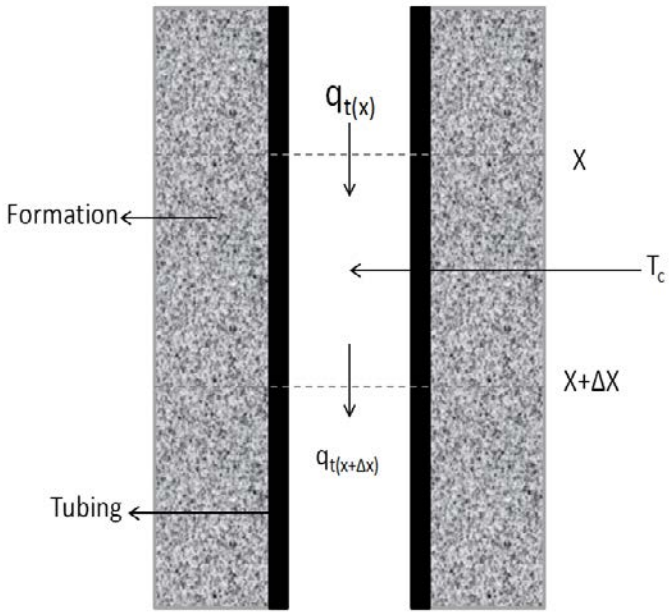

Fig. 3.3 Schematic of heat transfer to CO_2 in a wellbore.

Eq. (3.2) is solved by Arnold (1990) with an analytical approach for drilling mud. However, this approach cannot be used for CO_2, because CO_2 thermodynamic behavior and its properties are totally

different from drilling mud. To solve this intricate problem, a novel approach is suggested. First the equation is solved while considering the thermodynamic behavior of CO_2. Then the variations in thermal conductivity and specific heat values of CO_2 with the change in depth, and temperature are accounted.

CO_2 temperature is based on the principle of heat transfer and is determined by the rate of heat convection down the tubing, considering the change in specific heat. CO_2 temperature in the tubing is computed by the rate of heat exchange between the tubing and the formation, and by the rate of convection down the tubing. The solution is based on the following assumptions:

1. Axial heat conduction for CO_2 is negligible compared to its radial convection.
2. In the tubing, there is no radial temperature gradient.
3. The formation is assumed to be radially symmetric and infinite with respect to heat flow.
4. It is assumed that CO_2 in the supercritical conditions is incompressible.
5. The heat generated by fluid friction and viscous forces is negligible.

The temperature of CO_2-rock interface is determined from heat balance from the tubing to the formation per unit length.

$$Q = 2\pi r_t U_f (T_c - T_f) = \frac{2\pi k (T_f - T_g)}{f(t_D)} \qquad (3.3)$$

Where, U_f is the overall heat transfer coefficient between the tubing and the formation in KJ/hr-m^2-^oC, T_c and T_f are the temperatures of the CO_2 and the formation in ^oC, respectively. T_g is the initial geothermal temperature and $f(t_D)$ is a dimensionless time function proposed by Ramey (1962). These equations are used for CO_2 considering the variation in its thermodynamic behavior and change in its properties, and derived the following equation.

$$T_c = a_1 e^{zb_1} + a_2 e^{zb_2} + T_s - Xg + zg \qquad (3.4)$$

Where, the following constants are for CO_2 temperature prediction in the tubing and to calculate its temperature at a specific depth.

$$X = \frac{mc_{pi}}{2\pi r_t U_t}$$

$$Y = mc_{pi}[r_t U_f f(t_D) + k_f]$$

$$a_1 = \frac{(T_s - T_{se} + X_g)b_2 e^{b_2 z_t} + g}{b_2 e^{b_2 z_t} - b_1 e^{b_1 z_t}}$$

$$a_1 = \frac{(T_s - T_{se} + X_g)b_1 e^{b_1 z_t} + g}{b_1 e^{b_1 z_t} - b_2 e^{b_2 z_t}}$$

$$b_1 = \frac{1 + \left(1 + \frac{4Y}{X}\right)^{1/2}}{2Y}$$

$$b_2 = \frac{1 - \left(1 + \frac{4Y}{X}\right)^{1/2}}{2Y}$$

The experimentally determined thermodynamic properties of CO_2 are updated in the simulator with the change in depth and temperature. As a result, it gave accurate temperature of CO_2 for deep and shallow wells.

By analyzing CO_2 injection temperature profiles in detail, it is found that CO_2 temperature profile behaves non-linearly near the surface and at the exit from the tubing as shown in Fig. 3.4. Near the surface, it happens due to the fact that the injection temperature of CO_2 is 31.1°C, while the surface temperature is 26°C. Therefore, injected carbon dioxide loses some of the heat to the surroundings. At the exit from the tubing, fluid expansion and turbulence cause an additional loss of heat. This finding demonstrates over-all trend of temperature profile in the wellbore during CO_2 injection.

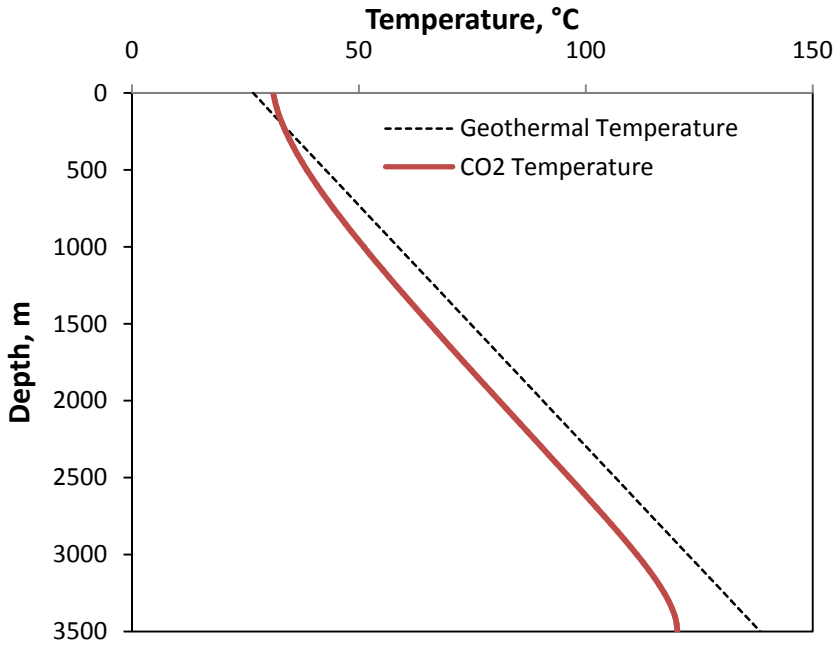

Fig. 3.4. Carbon dioxide temperature profile inside the tubing.

3.4 Validation and Comparison

After developing the thermal simulator, the results are compared with three set of observations to check the accuracy and precision in temperature prediction. At first simulated CO_2 temperature profiles is compared with the drilling mud temperature profile, then with field measured temperature data of drilling mud, and at last with CO_2 field measured data.

It is assumed in the simulation study that the wellbore diameter and all the drilling parameters are constant as shown in Table 3.1 except for the CO_2 thermal properties.

Table 3.1 Well and formation properties

Well Geometry	
Total depth, m	3500
Thermal conductivity of the formation, KJ/hr-m-^oC	8.1
Specific heat of the formation, KJ/kg-^oC	0.88
Equivalent surface temperature of the formation, ^oC	26.67
Geothermal gradient, ^oC/m	0.0292
Thermal conductivity of tubing and casing, KJ/hr-m-^oC	156
Heat transfer coefficient b/t conduit and annulus, KJ/hr-m^2-^oC	500
Heat transfer coefficient b/t annulus and formation, KJ/hr-m^2-^oC	400
Thermal diffusivity of formation, m^2/hr	0.0035
Inner diameter of tubing, m	0.048
Outer diameter of tubing, m	0.058

Fig. 3.5 shows the comparison of temperature profile for CO_2 and drilling mud. It can be noted that there is a big difference in the temperature of the both fluids. The difference occurs mainly due to

accounting and updating the change in thermodynamic fluid properties in the simulator.

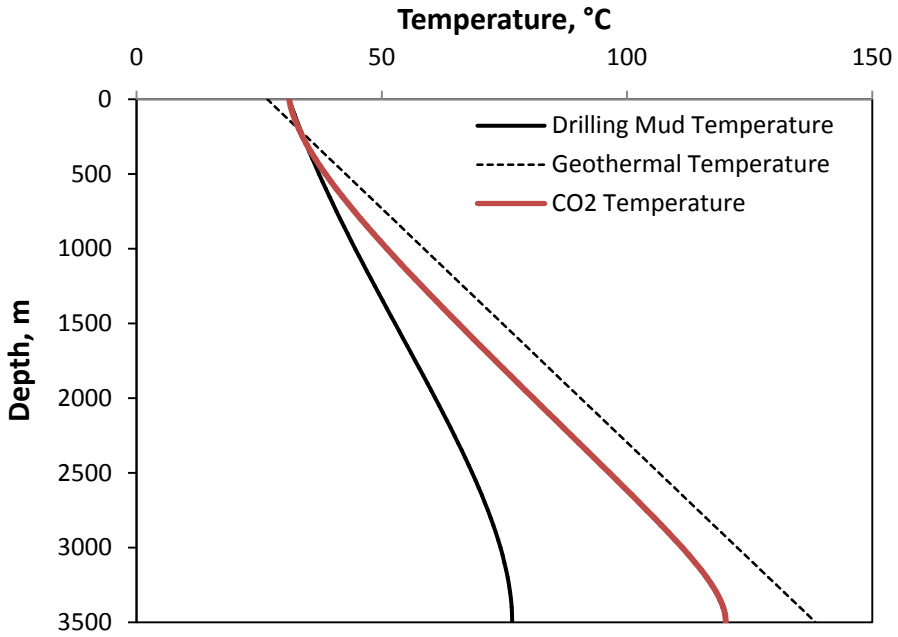

Fig. 3.5 Comparison of carbon dioxide and drilling mud temperature profile.

It is found that with the increase in depth and temperature, the change in viscosity, thermal conductivity, and specific heat of drilling mud remains low because drilling mud is a mixture of thermally inert materials. The results also demonstrate that CO_2 temperature profile goes along with the geothermal temperature as CO_2 thermodynamic properties are sensitive to its temperature. Hence, updating CO_2 properties for a degree rise in the temperature leads to convincing results.

Fig. 3.6 shows comparison of CO_2 temperature with drilling mud field measured thermal data (Stiles and Trigg, 2007). The temperature profile of drilling mud obtained by the developed simulator proves the accuracy of the simulator. Table 3.1 shows input data used for the comparison and validation of the model.

Fig. 3.7 shows the validation and comparison of predicted CO_2 temperature with CO_2 field measured data. It demonstrates the effect of using CO_2 thermodynamic properties and results in a good temperature match.

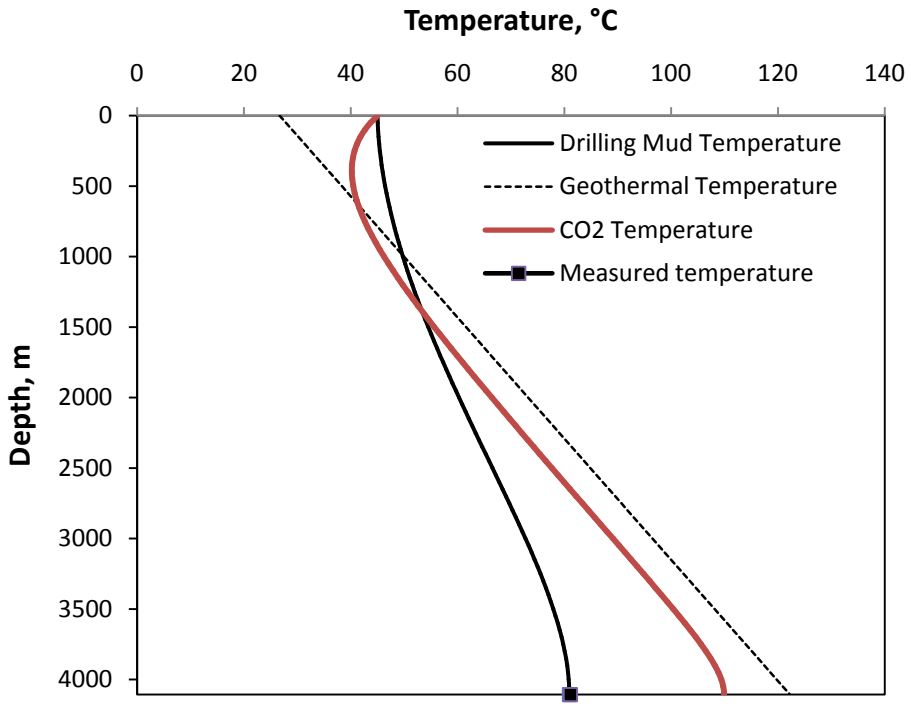

Fig. 3.6. Simulator comparison with field measured data from Stiles and Trigg (2007).

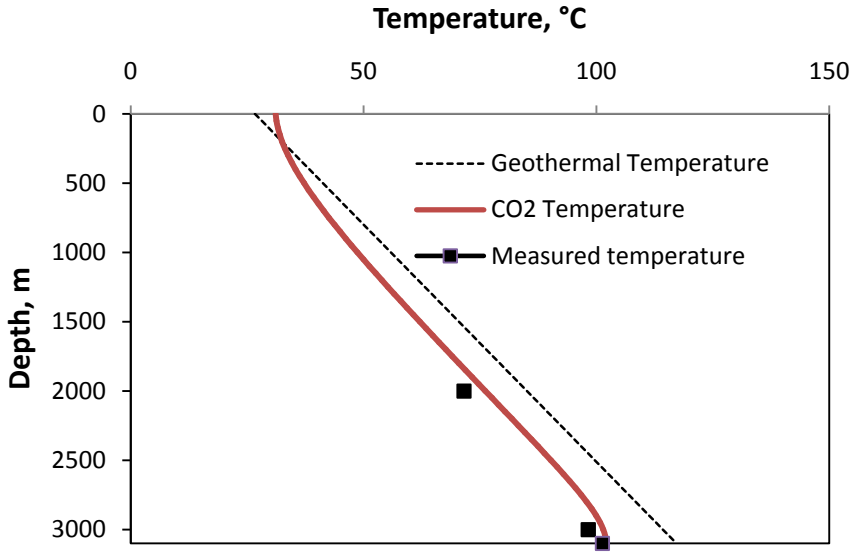

Fig. 3.7 Comparison with field measured data from Yong and Renxuan (2007).

Table 3.2 shows input data of CO_2 used for the comparison and validation of the model. The predicted CO_2 temperature at the reservoir depth of 3100m is 102.04°C, while at the same conditions the measured temperature of CO_2 by Yong and Renxuan (2007) was 103.14°C. The error is about 1.07%, which shows a reasonable agreement.

Table 3.2 Data for comparison and validation of CO_2 temperature

Well Geometry	
Total depth, m	3100
Thermal conductivity of the formation, KJ/hr-m-°C	8.1
Specific heat of the formation, KJ/kg-°C	0.88
Equivalent surface temperature of the formation, °C	26.67
Geothermal gradient, °C/m	0.029
Thermal conductivity of tubing and casing, KJ/hr-m-°C	156
Heat transfer coefficient b/t conduit and annulus, KJ/hr-m^2-°C	500
Heat transfer coefficient b/t annulus and formation, KJ/hr-m^2-°C	400
Thermal diffusivity of the formation, m^2/hr	0.003

The comparison of using updated and constant CO_2 values is shown in Fig. 3.8. It can be observed that, there is a big difference for the temperature predictions by updating thermodynamic properties rather than using constant values. The suggested approach shows an error of 1.07%, while previous studies have more than 12% (Romero and Touboul, 1998; Hasan and Kabir, 2002). Therefore, this approach works efficiently and reduces errors in CO_2 temperature prediction.

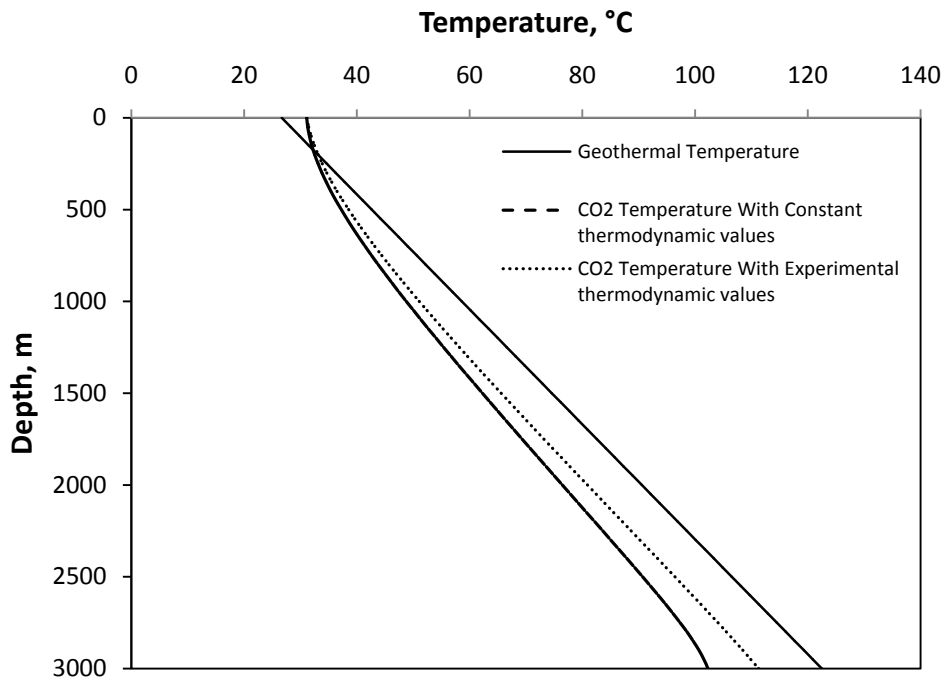

Fig. 3.8 Comparison for the use of experimental determined and constant thermodynamic properties of CO_2.

3.5 Factors Affecting CO_2 Temperature

To understand and design CO_2 injection parameters in a reliable manner, this study performs sensitivity analyses of a number of injection parameters. It is found that the parameters that play a key role in CO_2 temperature prediction are geothermal gradient, injection rate, injection time and surface temperature.

3.5.1 Effect of Geothermal Gradient

The geothermal gradient of the earth is not constant everywhere on the globe. At some places it is high and at some place it is low. The objective of analyzing the effect of geothermal gradient is to know, how it affects the CO_2 temperature. It is observed that, when the flow of heat is high in high geothermal gradient area, the temperature of CO_2 will rises and vice versa as shown in Fig. 3.9. In all the simulations the surface temperature, CO_2 injection temperature, and injection rate were kept constant at 26.7^{o}C, 31.1^{o}C, and 200 gpm, respectively while the geothermal gradient varies.

The results demonstrate that CO_2 temperature at the bottom of the well at 3500m depth are 100.3, 107.8, and 128.1^{o}C at the geothermal gradient of 0.023, 0.0255, and 0.0319^{o}C/m, respectively. Therefore, whenever it is planned to sequester CO_2 in an area with high geothermal gradient, the temperature of injected CO_2 must be analyzed in detail. So that proper and recommended practices may be applied.

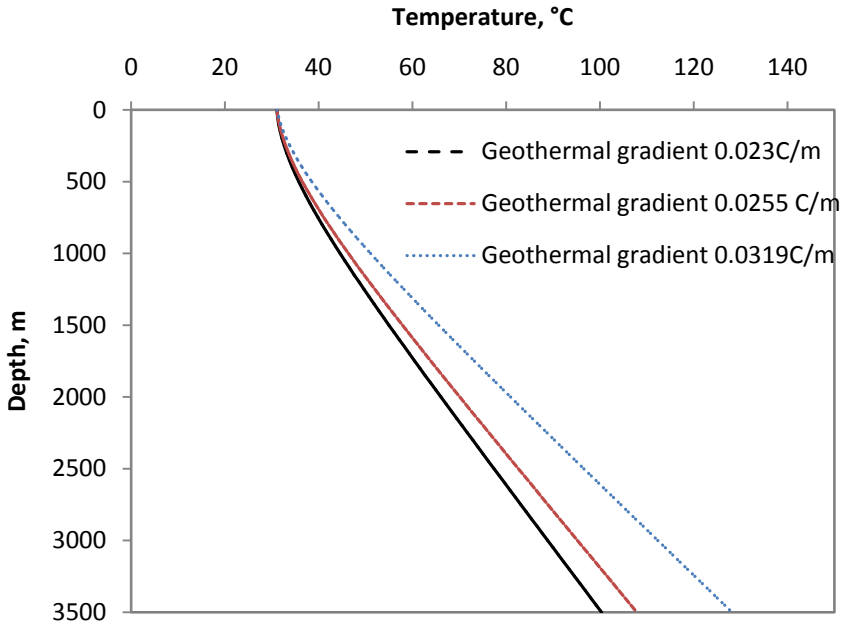

Fig. 3.9 Effect of geothermal gradient.

3.5.2 Effect of Injection Rate

Fig. 3.10 presents the influence of injection rate on CO_2 temperature in the wellbore. It can be observed that when CO_2 is injected at a low rate. Its temperature remains close to the geothermal formation temperature, because the injected CO_2 has much more time to interact with the surrounding formations. Thus it absorbs most of the heat from the formation.

When the injection rate is increased, CO_2 temperature profile remains low because high injection rate gives less time of interaction with the surroundings. However, at low injection rate CO_2

temperature will be high at the bottom of the well because of more time to interact. Therefore, proper injection rate should be selected.

It is important to explain very important issue regarding CO_2 injection which is usually ignored and confused: That is injection time and injection rate of CO_2. These two variables are different but result in dependent effect. Injection time is the duration of CO_2 injection in the wellbore while injection rate controls the velocity of CO_2. There is an inverse relationship between them.

High injection rate decreases the injection time for a planned amount of CO_2. If the injection rate is increased, carbon dioxide will break through quickly resulting in early recycling and lower sweep efficiency for enhanced oil recovery (EOR) projects. However, low circulation rate result in long injection time and elevated temperature of CO_2. Therefore, an optimum CO_2 injection rate must be selected to have minimum impact on reservoir properties.

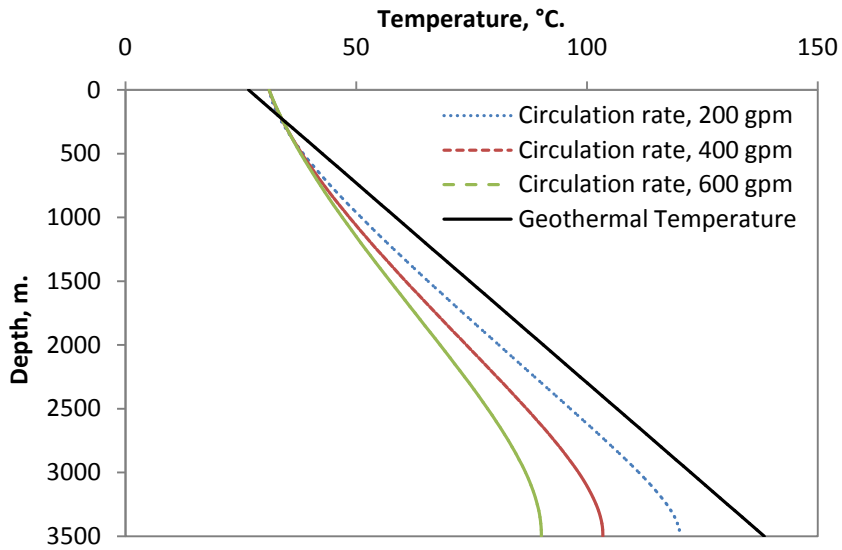

Fig. 3.10 Effect of injection rate.

3.5.3 Effect of Surface Temperature

The surface temperature is an important parameter. In the analysis of surface temperature, the CO_2 injection temperature, its rate, and formation geothermal gradient are kept constant at 31.1°C, 200 gpm, and 0.0292°C/m, respectively, while the surface temperatures are 15, 25, and 35°C.

Fig. 3.11 reveals big differences in the temperature profile at the bottom of the wellbore. When the surface temperature is 15°C, the CO_2 temperature profile takes a curve path in the start, which implies heat transfer from the carbon dioxide to the surroundings. However, when the surface temperature is 35°C, the CO_2 temperature shows linear trend, starting from the surface as the carbon dioxide continuously absorbs heat from the formations until it reaches the reservoir.

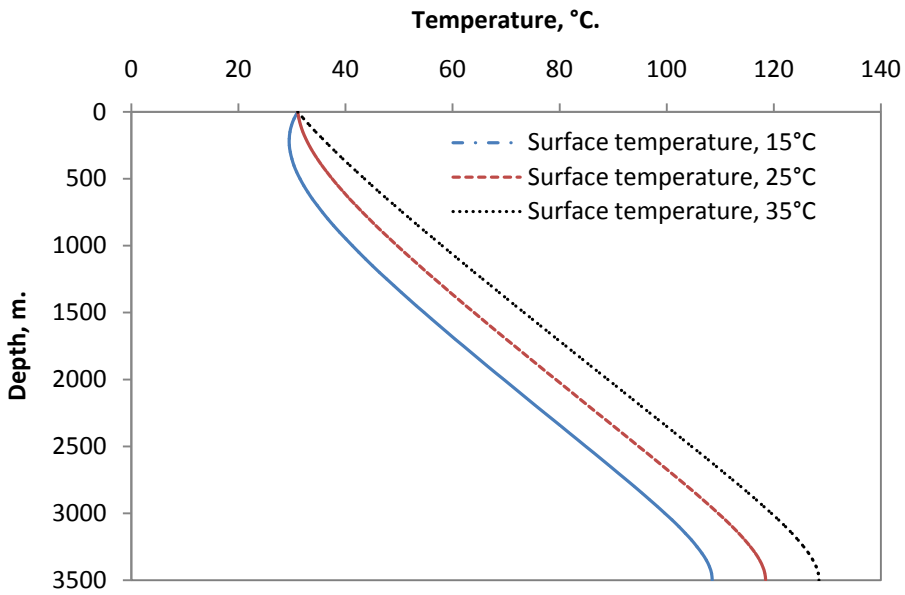

Fig. 3.11 Effect of surface temperature.

3.6 Results and Discussions

As mentioned accurate temperature prediction is important, because it directly affects chemical reactions in a reservoir. Fig. 3.12 shows porosity change for a reservoir at 2600m. It can be found that there is an ample difference with and without considering CO_2 thermodynamic properties. Therefore, it is important to predict accurate temperature of CO_2 for deep reservoirs to minimize the formation damages, in a better way.

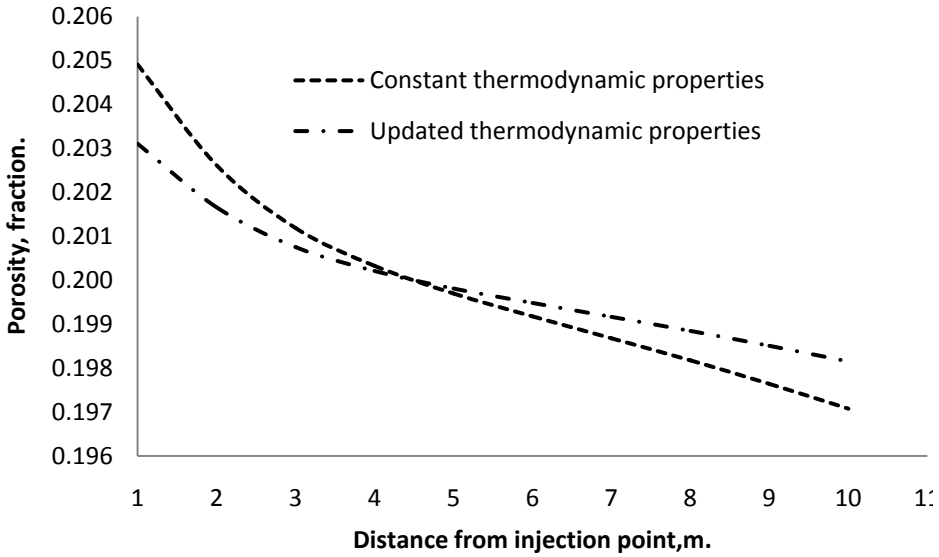

Fig. 3.12 Porosity variations and effect of using CO_2 thermodynamic properties.

The developed simulator was used to predict the temperature of CO_2 at different depth of 1000, 1800, 2600, 3400, and 4200 meters, respectively. Then these predicted values were used to estimate the formation damage (in detail in chapter 4). Fig. 3.13 shows the

comparison of porosity change due to CO_2-water-rock dissolution and precipitation at different CO_2 temperatures.

It can be observed that the dissolution and precipitation are high in shallow depth, because the dissolution reaction for carbonates minerals is exothermic. Thus the rate of dissolution increases at low temperature, as CO_2 has high solubility at low temperature and less at high temperature. This phenomenon slows down the carbonate dissolution reactions at high temperature (Matter and Kelemen, 2009).

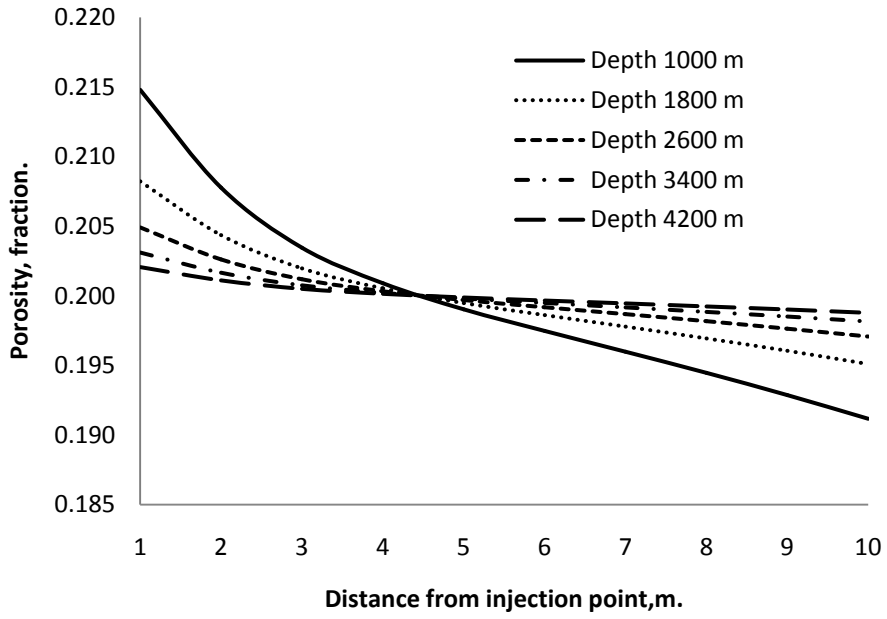

Fig. 3.13 Porosity variations and effect of CO_2 injection at different depths.

Regarding the precipitation of carbonates, it is observed that increased temperature decreases the precipitation of calcium carbonate and vice versa. In other words, when the temperature of a reservoir is high, the carbonate dissolution will be low and the

dissoluted particles will remain soluble in the media, leading to low formation damages.

It can be seen in Fig. 3.13, deep reservoirs are good candidate for CO_2 injection than shallow reservoirs as they get low formation damage during CO_2 injection. Accordingly, it is very important to know the accurate temperature of CO_2 at a given depth as it plays a decisive role to select the suitable precautionary measures to control the intensity of reactions that may take place in the reservoir.

3.7 Summary

1. The effect of temperature is usually neglected. However, the temperature of CO_2 is not typically same as geothermal gradient. It is a function of injection rate, injection time, geothermal gradient, and surface temperature.
2. The developed simulator with the proposed approach of using experimental determined specific heat values can be used as an efficient tool to predict thermal disturbances and to control dynamic behaviors of injected CO_2 to handle its injection performances in shallow or deep reservoirs**.**
3. The thermal and chemical impacts of CO_2 injection can be minimized by controlling CO_2 injection rate, time, and its surface temperature.
4. From the CO_2 reactive modeling, it is evident that the porosity increases significantly in the near wellbore region due to dissolution. It is also illustrated that temperature of CO_2 and its

injection rate control the mineral precipitation and spatial reactivity in a reservoir.

5. It is observed that deep oil and gas reservoirs are good candidates for CO_2 sequestration than shallow reservoirs because of low formation damages.

Chapter 4

FORMATION DAMAGE BY CO_2 INJECTION: ASPHALTENE DEPOSITION, CARBONATE DISSOLUTION AND PRECIPITATION, WITH THEIR CEMENTATION

4.1 Formation Damage

CO_2 EOR and its sequestration is becoming popular in subsurface geological structures specially depleted fields in controlling CO_2 emissions and enhanced oil recovery (EOR). In EOR operations CO_2 is known for its unique ability to displace oil from the reservoir rock, as a number of gases are tested for EOR after waterflooding. However, CO_2 remains the only candidate having the ability to reduce residual oil saturation to minimum and to produce significant amount of oil under both miscible and immiscible phase conditions (Lake, 1989). The benefits of CO_2 injection are so promising that its injection looks economically feasible. Even so, CO_2 injection in depleted reservoirs hides a number of reservoir engineering problems mainly formation damages and CO_2 mobility control (Khurshid and Choe, 2014c).

Formation damage is permeability impairment of the producing formation caused by various adverse processes. The processes include physical, chemical, thermal, and biological interactions of formation and injected fluids (Civan, 2000). While mobility control problems are: CO_2 early breakthrough and its unstable flow in the reservoir leading to viscous fingering and low sweep efficiency.

In case of CO_2 EOR and sequestration in depleted hydrocarbon reservoirs, its fluids and reservoirs conditions are different from those of aquifers. Thus, when CO_2 is injected in depleted reservoirs, it changes flow and phase behavior of reservoir fluids. It also disturbs the equilibrium of reservoir fluids by changing compositions, pH, and temperature leading to asphaltene deposition, formation of immobile gas, and reducing the relative permeability of oil and water.

A number of researchers performed experimental investigation and developed models for asphaltene deposition in porous media (Gruesback and Collins, 1982; Srivastava et al., 1999; Wang and Civan, 2001; Zanganeh et al., 2012). This asphaltene deposition may change the rock wettability and reduce oil productivity and CO_2 injectivity.

The injected CO_2 not only causes asphaltene deposition but also reacts with formation leading to rock dissolution. Similarly a number of researchers performed experiments and developed models to predict CO_2 dissolution process. Gaus et al. (2008) performed geochemical and solute transport modeling of CO_2 and showed that CO_2 injection increases saline water acidity leading to carbonate dissolution in the near wellbore region.

Wang et al.(2011) mentioned that the condensable impurities in CO_2 stream increase storage capacity, while the non-condensable impurities increase the buoyancy. André et al. (2009) studied the thermal impact of supercritical CO_2 and analyzed its chemical reactivity in a carbonate saline aquifer. Matter and Kelemen (2009) mentioned that the CO_2 solubility decreases with increasing

temperature and water ionic strength. Zeidouni et al. (2009) modeled the salt precipitation in saline aquifer during CO_2 injection and evaluated the effect of salt precipitation.

Dulov (2011) simulated CO_2 injectivity by developing a cylindrical-cone model and showed that these dissoluted particles may cause well plugging. Khurshid and Choe (2013) performed sensitivity analysis of CO_2 injection parameters and illustrated that the geothermal gradient, CO_2 injection rate, and surface temperature are the most important parameters during sequestration activities.

To determine the amount, magnitude, and extent of irreversible formation damages during CO_2 EOR, it is important to develop a model that combines the rate of asphaltene deposition, rock dissolution, and precipitation of the dissoluted particles (Khurshid and Choe, 2014c). Therefore, in this study a model is developed to simulate the rock dissolution, asphaltene and carbonate particles precipitation as a function of time and space. This technique and concept of cementation is not utilized before to characterize the irreversible formation damage phenomenon. This approach gave us the prediction of formation damage for CO_2 injection activities. Fig. 4.1 shows the flowchart for formation damage analysis used in this study.

In this study sensitivity analysis of different injection parameters is also performed to control the formation damage. The results shows that developed methodology can be used as a cost effective and an efficient tool to monitor the dynamic behavior of CO_2, and control its reactivity and formation damages.

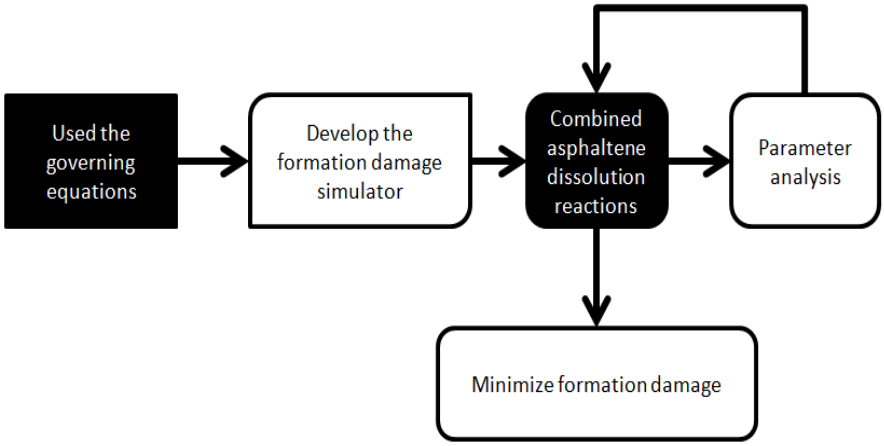

Fig. 4.1 Flowchart for formation damage analysis.

4.2 Physics of the Problem

Consider a radial model in which CO_2 is injected in an infinitely large reservoir through a well in the centre of the reservoir. The following is a possible phase arrangement: deep in the reservoir, where formation fluids has not been in contact with injected CO_2, only heavy hydrocarbon mainly asphaltene exists in the region as evident from Fig. 4.2 In the upstream a zone of three components (carbonic water, carbonates and asphaltene) develops (region 2 in Fig. 4.2). At a certain point in region 2 (cementation zone), the phase flows slowly such that the dissoluted particles gain terminal velocity and settle down on the deposited sticky asphaltene leading to cementation. The saturation of carbonated water and carbonates increases toward the injection well. Further towards the injection well is the dissoluted zone, where the fresh injected CO_2 interacts with water forming carbonic water (carbonic acid) and it chemically

interact with reservoir rock leading to rock dissolution. This process creates a dissoluted zone (region 3) in the near wellbore area.

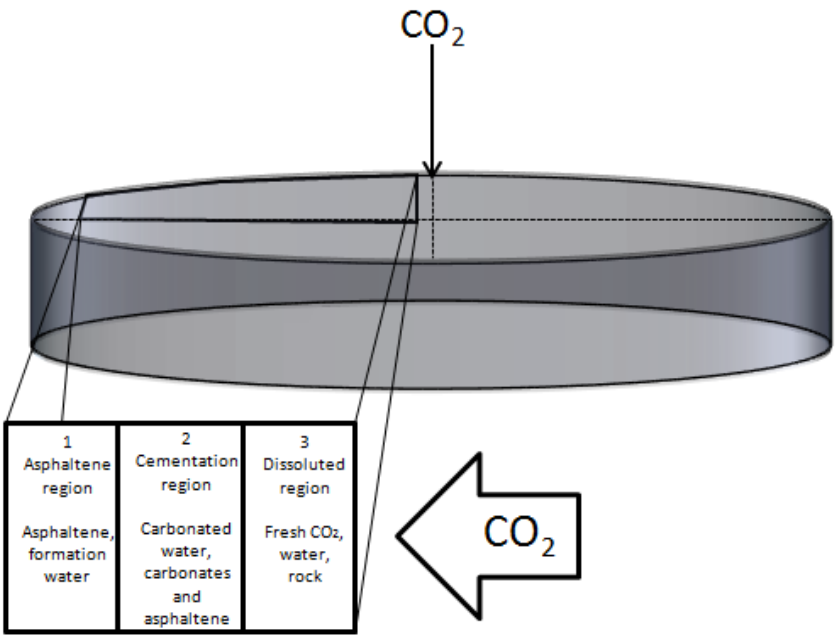

Fig. 4.2 Schematic of CO_2, water, rock interaction and different phases.

4.3 Formation Damage Model

To develop a formation damage model for asphaltene and carbonate cementation, it is essential to determine 1) the deposition of asphaltene, 2) the source of chemical components, 3) transport of carbonate particles to the point of fixation, 4) precipitation of carbonate particles, and 5) the formation damage by considering the change in porosity and reduction of surface area available for CO_2 flow.

When CO_2 is injected in a reservoir for EOR after waterflooding, its flow in the reservoir is described by the continuity

equation, which is a partial differential equation describing the law of mass conservation for every point in the porous media. The continuity equation for oil, gas, and aqueous phase are

$$\frac{\partial(\rho_o u_o w_o)}{\partial r} + \frac{\partial(A\phi\rho_o S_o w_o)}{\partial t} = 0 \tag{4.1}$$

$$\frac{\partial(\rho_g u_g w_{go})}{\partial r} + \frac{\partial(A\phi\rho_g S_g w_g)}{\partial t} = 0 \tag{4.2}$$

$$\frac{\partial(\rho_a u_a w_a)}{\partial r} + \frac{\partial(A\phi\rho_a S_a w_a)}{\partial t} = 0 \tag{4.3}$$

Where, the summation of equations 4.1 to 4.3 gives:

$$-\frac{\partial}{\partial r}\left(\rho_o u_o w_o + \rho_g u_g w_g + \rho_a u_a w_a\right) = \frac{\partial}{\partial t}\left(A\phi\rho_o S_o w_o + A\phi\rho_g S_g w_g + A\phi\rho_a S_a w_a\right) \tag{4.4}$$

For the CO_2 component neglecting diffusion, the equation for all the phases is,

$$-\frac{\partial}{\partial r}\left(\rho_o \omega_{CO_2,o} u_o w_o + \rho_g \omega_{CO_2,g} u_g w_g + \rho_a \omega_{CO_2,a} u_a w_a\right) = \frac{\partial}{\partial t}\left(A\phi\rho_o \omega_{CO_2,o} S_o w_o + A\phi\rho_g \omega_{CO_2,g} S_g w_g + A\phi\rho_a \omega_{CO_2,a} S_a w_a\right) \tag{4.5}$$

Where by considering constant injection rate, eq. 4.5 can be written as

$$-\frac{q_{inj}}{A\phi}\frac{\partial}{\partial r}\left(\rho_o\omega_{CO_2,o}u_o w_o+\rho_g\omega_{CO_2,g}u_g w_g+\rho_a\omega_{CO_2,a}u_a w_a\right)=$$

$$\frac{\partial}{\partial t}\left(\rho_o\omega_{CO_2,o}S_o w_o+\rho_g\omega_{CO_2,g}S_g w_g+\rho_a\omega_{CO_2,a}S_a w_a\right)$$

(4.6)

The mass balance for the asphaltenes can be given as

$$\frac{\partial}{\partial t}\left(A\phi S_l\rho_{as}C_{as}+A\phi S_l\rho_l w_{as}\right)+\frac{\partial}{\partial r}\left(\rho_l u_l w_{as}+\rho_l u_l w_{as}\right)=-\rho_{as}\frac{\partial V_{as}}{\partial t}$$

(4.7)

Where ρ is the density in kg/m^3, *u* is the CO_2 flow rate in kg/s, A is the area in m^2, S is the saturation in percent, ϕ is the porosity in percent, *w* is the mole concentration, V is volume in m^3 and t is time in s. Subscripts a, o, g, as are aqueous, oil, gas, and asphaltene, respectively.

Rate law and Chemical Reactions: In order to model asphaltene deposition in porous media, Gruesbeck and Collins (1982) developed a model for fine particles deposition in single phase flow, and found that the deposition rate is directly related to the concentration of fine particles in the fluid. Civan (2000) improved their formulation and developed a model based on the asphaltene deposition, entrainment, and plugging.

Wang and Civan (2001) further improved the asphaltene deposition and showed that the net rate of asphaltene deposition is dependent on the asphaltene concentration, its saturation, and porosity. However, they also showed that the pore throat plugging is

directly proportional to superficial velocity μ_l, liquid saturation, and asphaltene concentration. They proposed the following equation.

$$\frac{\partial Z_{as}}{\partial t} = \alpha_{as} S_l C_{as} \phi - \beta_{as} d_{as} \left(v_l - v_{cr.l} \right) + \gamma u_l S_l C_{as} \tag{4.8}$$

Where Z_{as} is the net asphaltene deposition, α_{as} is the coefficient for asphaltene surface deposition, S_l is the liquid saturation in percent, C_{as} is the asphaltene concentration in weight percent, ϕ is the porosity, β_{as} is the asphaltene entrainment rate coefficient in 1/cm, v_l is interstitial velocity cm/s, γ is the plugging deposition rate coefficient in 1/cm and μ_l is the superficial velocity.

Consequently, when asphaltene deposits in a porous media around a grain, it blocks the flow paths. In case of multiphase flow, increasing temperature decreases the heat transfer. This decrease in heat transfer increases the rate of asphaltene deposition in porous media. Because in a chemical reaction the deposition of a particle depends on the concentration of reactant, and is inversely related to the velocity of reactant. Therefore, the aforementioned description for asphaltene deposition is described in the following equation (Soulgani et al., 2011).

$$\frac{\partial d_{as}}{\partial t} = K \frac{C_{as} e^{-E/RT}}{v} \tag{4.9}$$

Where d_{as} is asphaltene deposition rate per unit time, K is the reaction rate coefficient, C_{as} is the concentration of asphaltene in percent, E is the activation energy in J/mol, R is the universal gas

constant in J/mol*K, T is the reservoir temperature in K, and ν is the CO_2 flow rate in kg/hr.

When CO_2 is injected continuously, it dissolves in the aqueous phase, reacts with the reservoir water and forms carbonic acid. At the same time carbonic acid dissociates and forms bicarbonate ions. These bicarbonate ions dissociate to form carbonate and hydrogen ions. They then react with the carbonate rock and the rock disintegrates into fine particles. These particles after attaining terminal velocity precipitate on the already deposited asphaltene in the porous media, leading to pore plugging. The relationship between CO_2, calcium and bicarbonate ions, and their precipitation are described by the following reactions (André et al., 2007).

$CO_{2\,(g)} + H_2O \leftrightarrow HCO_3$

$HCO^-_3 \leftrightarrow H^+ + CO_3^{2-}$

$CaCO_3 + H^+ \leftrightarrow 2HCO^-_3 + Ca^{2+}$

$Ca^{2+} + CO_3^{2-} \leftrightarrow CaCO_3$

The impact of above reactions on rock dissolution and asphaltene deposition is dependent on the rate of reaction. For this reason, numerical modeling with kinetic laws is used to access the impact of these geochemical reactions. The Arrhenius equation is utilized for the forward and the backward reactions, which is as follow

$$\frac{\partial Y}{\partial t} = K_f \nu e^{-E/RT} - K_b \frac{e^{-E/RT}}{\nu} \qquad (4.10)$$

Where, Y is the rate of reaction per unit time that will occur in the reservoir, ν is the CO_2 injection rate in kg/hr, K is the reaction rate

coefficient, E is the activation energy in J/mol, R is the universal gas constant in J/mol*K, and T is the reservoir temperature in K. The negative sign shows the precipitation. Subscripts f and b represent forward reaction and backward reaction, respectively. The equation (4.9) and (4.10) were combined to formulate the net reaction that will occur in the reservoir.

The mass conservation of carbonate particles in the porous media gives the following partial differential equation

$$\frac{\partial(\phi N)}{\partial t}+\frac{\partial(vN)}{\partial x}=-\phi p(N-\chi) \qquad (4.11)$$

Where ϕ is the porosity in fraction, N is the concentration of carbonates in the reservoir fluid in kg/kg, *v* is the rate of fluid flow, x is the distance from the injection point in the reservoir, p is the precipitation rate constant, and χ is the solubility of carbonate in kg/kg. We assume that in the start of CO_2 injection.

$$N(x,t=0)=\chi$$

The equation for carbonate particles over asphaltene during deposition gives the following relation between the rate of growth in V_c and the rate of carbonate particles removing out by V_r

$$\rho_c\frac{dV_c}{dt}=\rho_r V_r p(N-\chi) \qquad (4.12)$$

Where ρ_c is the density of carbonate in kg/m^3, V_c is volume of carbonate grains in m^3, ρ_r is the density of reservoir fluid in kg/m^3, V_r is volume of reservoir fluid in m^3, p is the apparent precipitation rate

constant, N is the concentration of carbonates in the reservoir fluid in kg/kg, and χ is the solubility of carbonate in kg/kg**.**

When carbonate rock after dissolution, disintegrates into carbonate particles. These particles are transported with the fluid flow to the point of fixation and they precipitate when they attain the terminal velocity. This velocity is defined as when the gravitational force acting downward, and the sum of drag and buoyancy force acting upward become equal and their sum is zero. Therefore, the motion of particles is governed by the following Smoluchowski equation.

$$\frac{\partial C_s}{\partial t} - \frac{\partial}{\partial x}\left[\frac{C_s}{F(x)}\frac{\partial E_P}{\partial x} + D(x)\frac{\partial C_s}{\partial x}\right] = 0 \qquad (4.13)$$

Where C_s is the particles concentration in suspension, E_p is the potential energy, F is the drag force coefficient, and D(x) is the diffusion coefficient.

In order to model the macroscopic rate of deposition, it is assumed that the potential energy is either attractive or repulsive. For this reason, the pore acts as perfect sinks or sources. Therefore, the rate of deposition of particles per pore volume per unit time is combined with the rate of carbonate growth in the porous media giving the following equation.

$$\frac{\partial d}{\partial t} = 2\pi D^{2/3} L^{2/3} C_s \int \left(r^2 \nu\right)^{1/3} f\left(p\right) dr \qquad (4.14)$$

This equation is similar to the particles deposition and release by Sharma et al., (1985) except for considering the concentration of particles in the pores, constant fluid velocity, and assuming that the length of pore is equal to pore radius. Therefore, the dissoluted particles precipitation in the porous media per pore volume per unit time after summation is given by.

$$\frac{\partial d}{\partial t} = 2\pi D^{2/3} v^{1/3} \sum_{i=1}^{n} r_i^{4/3} C_s f(p) \Delta r \qquad (4.15)$$

Where d is deposition rate per unit time, D is the diffusivity in the pores, L is the pore length in m, C_s is the concentration of particles in suspension in percent, r is the pore radius in m, *v* is the fluid velocity in kg/hr and f(p) is pore distribution function.

The more we inject CO_2, high rate of dissolution will occur in the near wellbore region. Thus, the particles will be deposited away from the wellbore on the already deposited asphaltene leading to cementation. Fig. 4.3 shows the schematic diagram of organic and inorganic particulates deposition in porous media.

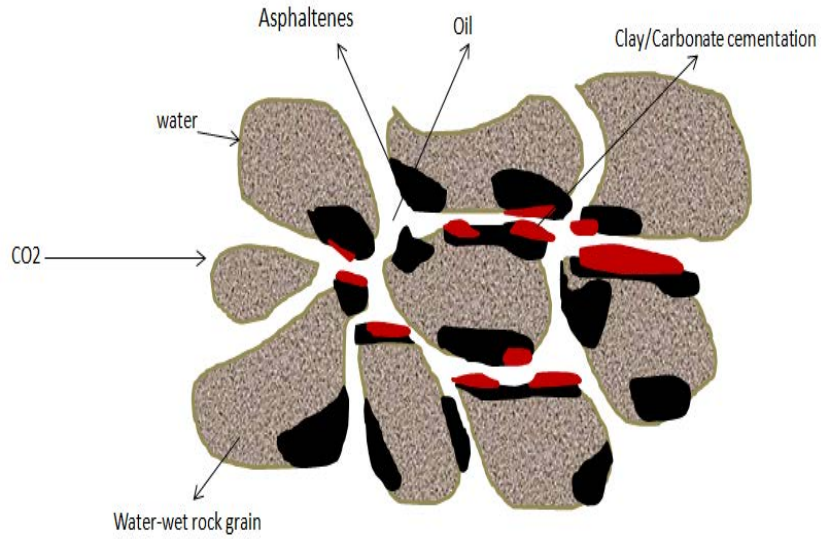

Fig. 4.3 Schematic of carbonate and asphaltene depositions.

4.4 Surface Area Modifications

During CO_2 injection the surface area of the porous media changes due to asphaltene and carbonate particles precipitation, and cementation thereafter. So, the porosity increases in the near wellbore region and decreases in the far region as described by equations (4.9)-(4.15). The cementation may affect the permeability of the porous media

$$\phi = \phi_i \left(1 - S_{cm}\right) \tag{4.16}$$

The Kozeny-Carman equation is used to describe the ratio of change in permeability to initial permeability and is determined by the following equation

$$\frac{k}{k_i} = \left(\frac{\phi}{\phi_i}\right)^c \left(\frac{1-\phi_i}{1-\phi}\right)^2 \qquad (4.17)$$

Where k is the permeability, ϕ is the porosity and S_{cm} is cement saturation. Subscripts i represents initial and exponent e has values of 3, 5, and 12 depending upon the clean formations, anhydrite precipitation, and for core flooding, respectively (Izgec et al., 2006). The equation (16) and (17) are combined and the following equation is derived to determine the reduction in permeability due to cementation.

$$\frac{k}{k_i} = \frac{\left(1-S_{cm}\right)^3}{\left(1+\left(\phi_i/\left(1-\phi_i\right)\right)S_{cm}\right)^2} \qquad (4.18)$$

4.5 Validation and Verification

The data from core flooding experiments are important to understand the effect of CO_2 injection. However, these experiments are not representative of reservoir conditions. Because CO_2 storage is a complex phenomenon depending on properties of host rock, composition of formation water, the thermodynamic conditions, and flow rate. So, CO_2 flooding experiments in small cores only simulate the near wellbore region.

Therefore, to validate the results with reservoir conditions the data from Bacci et al. (2011) are utilized. They used two cores for their flooding experiments. The first one imitates the near wellbore region while the second core represents region far away from the wellbore. Fig. 4.4 shows the comparison of simulation results with experimental data from Bacci et al. (2011), with first three cells representing first core and remaining three cells showing the second core. The experimental data by Bacci et al. (2011) showed 1.7% increase in permeability, while this study got 1.72%. Bacci et al. (2011) showed a permeability decrease 1.6% while 1.44% in this study. Therefore, the model results show good agreement.

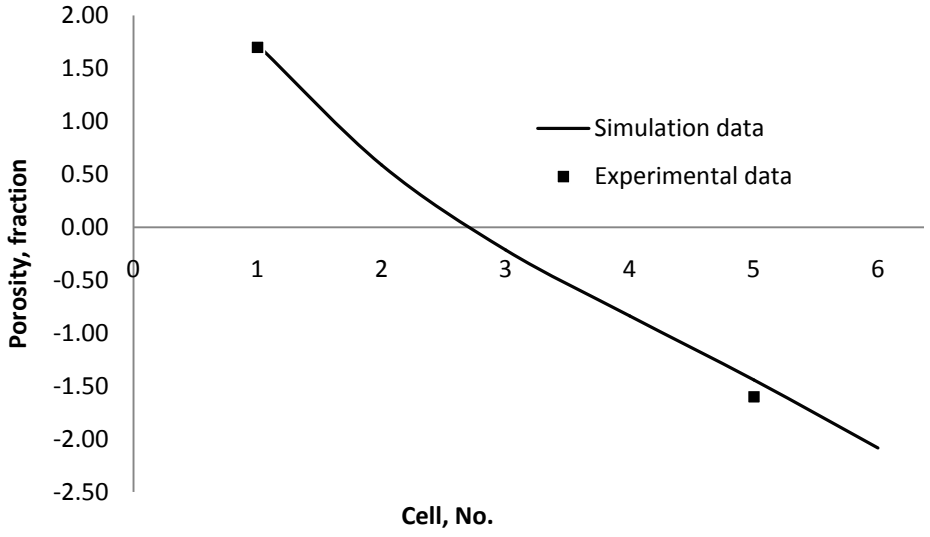

Fig. 4.4 Comparison of simulation results with experimental data from Bacci et al. (2011).

4.6 Factors Affecting Formation Damage and Cementation

The developed simulator is used to predict asphaltene and carbonate cementation as described in the previous sections. Different sets of reservoirs conditions are analyzed such as concentration of organic particulates, injection time, temperature, pressure, permeability, porosity, grain size, and particle size to characterize their effect. The values of these parameters were kept within the range representative of natural conditions as shown in Table 4.1. The simulations ran over a preset period of time, and then the changes in porosity and permeability are examined.

The effect of CO_2 injection time, temperature, injection rate, and particle size distribution are investigated in detail to analyze their effect. The results of different simulations are shown in the plots with porosity and distance from the CO_2 injection point. It is assumed that, initially the reservoir porosity is uniform throughout the reservoir.

Table 4.1 Physical properties of a reservoir used for formation damage modeling

Parameter	**Value**
Porosity, %	20
Permeability, m^2	450E-15
Viscosity of CO_2, Pa.s	2E-6
Density of CO_2, kg/m^3	450
Density of $CaCO_3$, kg/m^3	2700
Gas Constant, J/mol.K	8.31
Inlet radius of model, m	0.06
Concentration of asphaltene in oil, %	0.053
Reaction coefficient of forward reaction	3E-9
Reaction coefficient for backward reaction	1E-10
Asphaltene deposition coefficient	4.65E-5
Length of the model, m	10

In the model the deposition of asphaltene and carbonate takes place over one another. Thus, the cementation at any point in the reservoir is equal to the loss of reservoir porosity. The results indicate that asphaltene and carbonate cementation are substantial and the dissolution, precipitation, and cementation occur with the time.

4.6.1 Effect of CO_2 Injection Time

Fig. 4.5 illustrates the effect of CO_2 injection time and elaborates the changes in the reservoir porosity due to asphaltene deposition, rock dissolution, and their cementation. In order to determine the effect of these changes with time, the simulation time is kept at 1, and 10 years as shown in Fig 4.5 (a) and (b) respectively.

In the simulations the initial porosity is 0.2, and T= 75^{o}C Fig. 4.5 shows an increase of the reservoir porosity in the near wellbore region and decrease in porosity towards the production well. André et al. (2007) from their experiments demonstrated that CO_2 injection could cause 90% increase in porosity. In this study same behavior is observed and it is found that this huge porosity increase can create vugs along the wellbore.

It can be observed from Fig. 4.5 (a) and (b), the effect of asphaltene absence and presence. The concentration of asphaltene was limited to just 5.3% in the reservoir fluid (Soulgani et al., 2011). The amount of rock dissolution in the near wellbore will be high for asphaltene absence case. Since CO_2 attacks the rocks directly,

because the rock is without any asphaltene deposition (surface coating). However, rock dissolution is low when asphaltene is present.

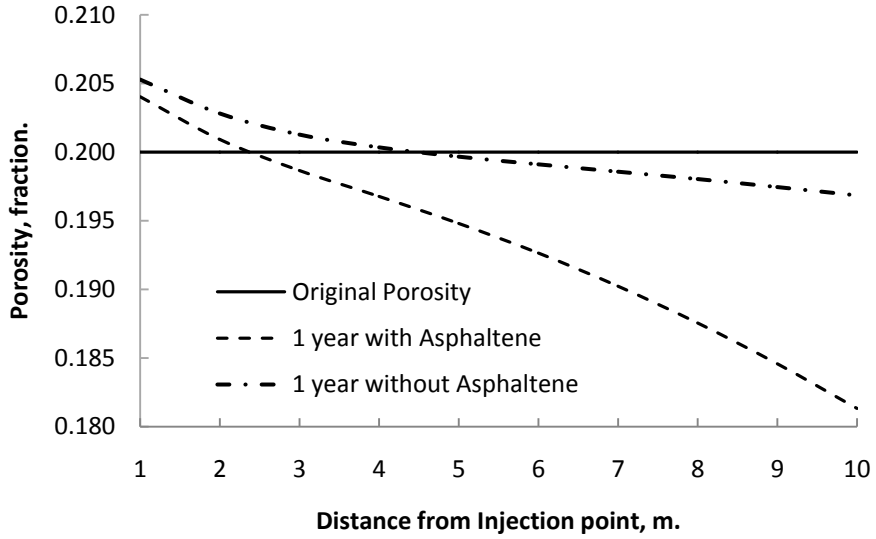

(a) After 1st year of injection

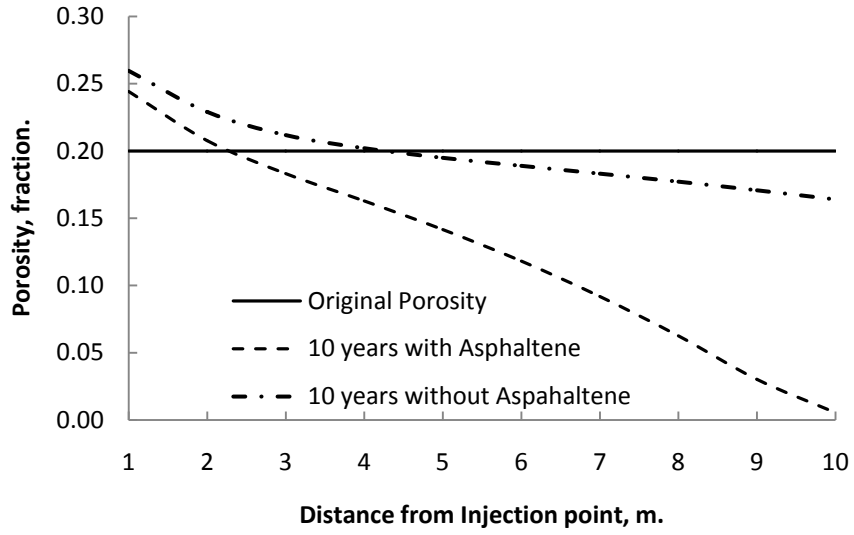

(b) After 10 years of injection

Fig. 4.5 Loss of porosity during calcium asphaltene cements vs the distance from the CO_2 injection point.

The reasons for low dissolution for the asphaltene presence case are: asphaltene deposits around the grains, where its deposition changes the rock wettability behavior. With continuous CO_2 injection, asphaltene is scratched and removed from the grains and then CO_2 interacts with the rock surface. After that, the dissoluted carbonate particles after attaining terminal velocity precipitates, adhere and cement on the deposited asphaltene resulting in decrease of porosity in high numbers. This overall process of asphaltene and carbonate cementation will lead to 80-90% decrease in porosity and permeability of the reservoir.

4.6.2 Effect of CO_2 Injection Rate

The effect of CO_2 injection rate is simulated to determine the extent of formation damage in the reservoir. Fig. 4.6 demonstrates the effect of CO_2 injection rate at 25, 50, and 75 kg/hr. The duration of flow is kept constant for one year with reservoir temperature of 75^{o}C. The results show that high flow rate decreases the reservoir porosity in elevated numbers. It can be noted that the extent of damage is low at low injection rate and it increases with increasing the injection rate.

The influenced area is directly proportional to CO_2 injection rate. It is observed that the amount of cementation increases in the reservoir from the injection well towards the production well. Therefore, a decrease in flow rate of CO_2 will result in reducing the carbonate dissolution and will help to reduce the dissolution,

precipitation and cementation. Therefore, it is important to select an optimum injection rate.

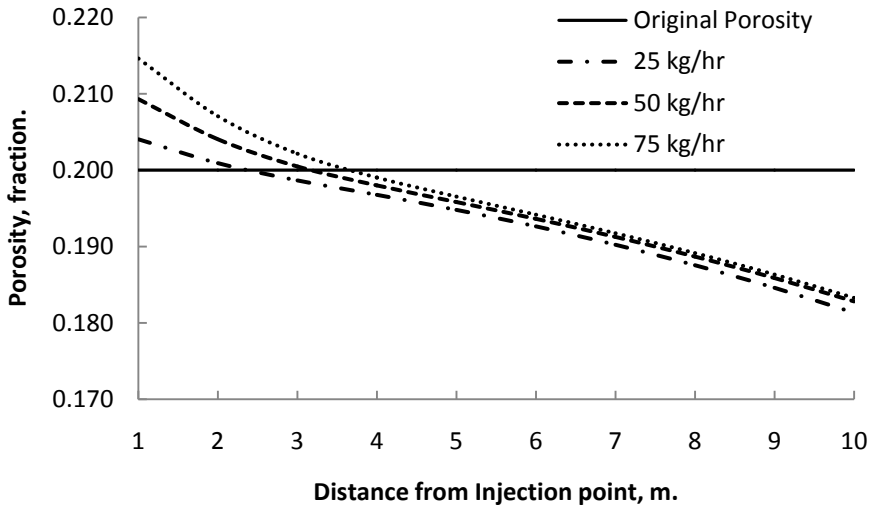

Fig. 4.6 Effect of injection rates on porosity change in the formation.

4.6.3 Effect of Reservoir Temperature

Fig. 4.7 shows the formation damages caused due to CO_2 injection at depths of 1000, 1800, 2600, 3400, and 4200 meters. It can be observed that the rate of dissolution and precipitation are high in shallow reservoirs. The reason is that the dissolution reaction for carbonates minerals is exothermic. Thus the rate of dissolution increases at low temperature, furthermore CO_2 has high solubility at low temperature and less at high temperature (Matter and Kelemen, 2009). Therefore, this phenomenon slows down the carbonate dissolution reaction at high temperature.

Regarding the precipitation of carbonates, it is observed that increasing the temperature decreases the precipitation of calcium carbonate and vice versa. Therefore, when the temperature of reservoir is high, the carbonate dissolution will be low and the dissoluted particles whether organic or inorganic will remain soluble in the media. Therefore, due to high temperature deep reservoirs are good candidate for CO_2 injection than shallow reservoirs.

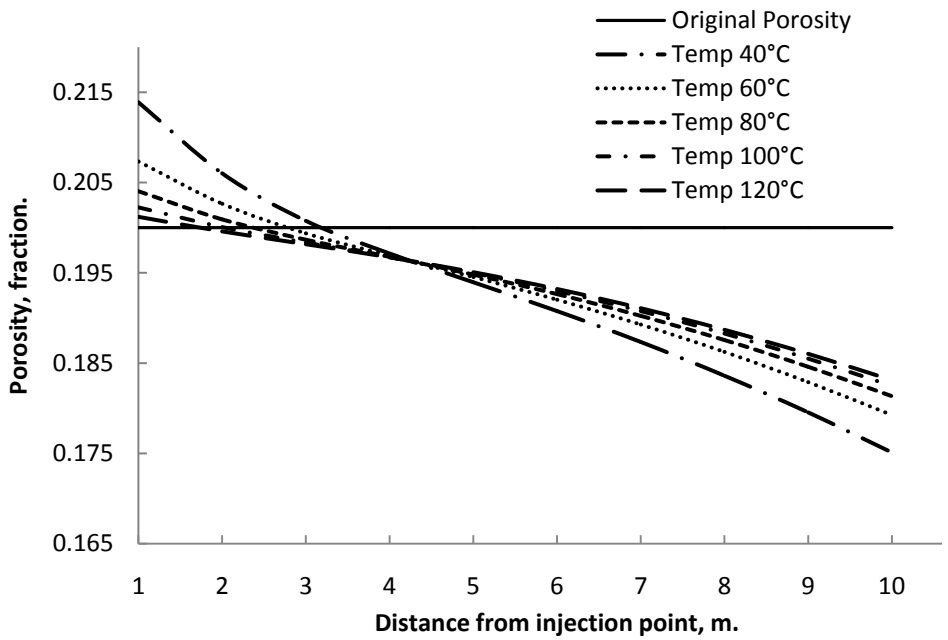

Fig. 4.7 Effect of reservoir temperature on porosity change in the formation.

Fig. 4.7 proves that, in terms of low formation damage during CO_2 injection, deep reservoirs are better than shallow reservoirs. However, injecting CO_2 in shallow reservoirs needs proper and appropriate injection parameters, as CO_2 may increase the dissolution reaction in the near wellbore region that may result in creation of

cavities around the wellbore. These cavities may increase stresses on the casing and lead to casing failure and wellbore stability problems.

4.6.4 Effect of Reservoir Heterogeneity

In the porous media detrital and diagenetic clays particles are distributed. Normal distribution is used to consider the effect of homogeneity and heterogeneity of these particles, and their particle size distribution. Four cases are modeled, to investigate the effect of these particles and their distribution on formation properties. The mean was kept 500 μm but standard deviations were changed from 200, 160, 120 and 80 μm. As a matter of fact high standard deviation shows heterogeneity.

Fig. 4.8 shows that formation dissolution is faster in heterogeneous particles than in homogenous particles because heterogeneous particles are less porous and has more surface area. Therefore, the injected CO_2 contacts and has large surface to react, resulting in high rate of formation dissolution, it can be observed in the case of 200 μm in Fig. 4.8.

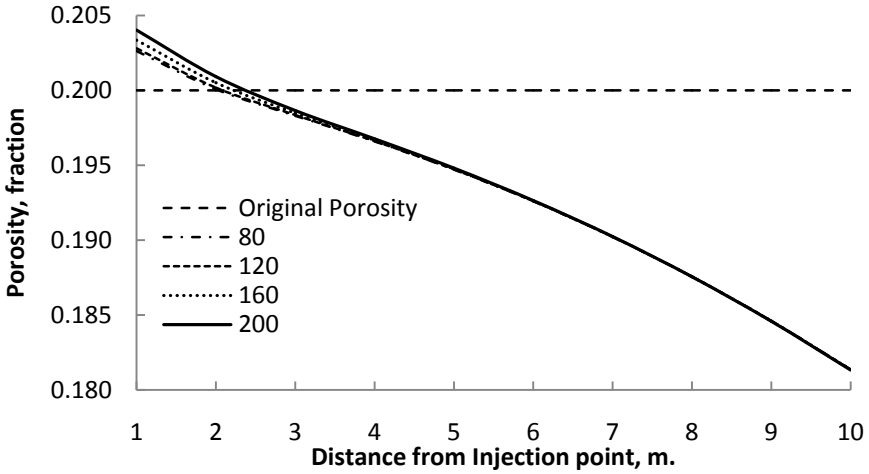

Fig. 4.8 Effect of particle size heterogeneity on porosity change.

4.7 Summary

1. A comprehensive simulator is developed that solves the fluid flow equations, chemical reactivity equations, and particles deposition equations. It considers the deposition of asphaltene, source of chemical components that take part in the carbonate dissolution reaction, transport of carbonate particles to the point of fixation, and precipitation.
2. The developed model also encircles the cementation of carbonate particles on asphaltene, and the change in porosity due to cementation. The model is validated with experimental data available and predicts the total extent of formation damage due to CO_2-rock-water-oil interactions.
3. It is observed that the consequences of asphaltene and carbonate precipitation are severe and it may lead to irreversible formation damage specifically cementation. This cementation may cause

permanent pore blockage leading to reduction of oil and gas productivity, and CO_2 injectivity.

4. In this study, it is found that the dissolution rate is high in shallow and heterogeneous formations, because low temperature conditions accelerate rock dissolution and deposition processes. On the other hand, high reservoir temperature causes an increase in the solubility of organic and inorganic particles leading to less damage.
5. Therefore, deep reservoirs are more competitive than shallow reservoirs for CO_2 sequestration. Thus, this formation damage simulator can be used as an efficient and cost effective tool to select a reservoir and can also help to control and minimize the formation damage giving maximum oil recovery and CO_2 storage.

Chapter 5

REDISSOLUTION AND REMOVAL OF DEPOSITED ASPHALTENE WITH INCREASING CO_2 STORAGE AND OIL RECOVERY

5.1 Asphaltene and its Deposition

With the decreasing trend of commercial discoveries, it is important to maintain high recovery efficiency. However, immense oil still remains in a reservoir after primary and secondary production (waterflooding). We can recover more oil by enhanced oil recovery (EOR) techniques. This residual oil is typically trapped by capillary forces. To reduce these forces, the best candidate is CO_2 at supercritical conditions. At supercritical conditions, CO_2 has density like a liquid but it mixes like a gas.

CO_2 for EOR activities mostly comes from geological traps, while only a small fraction is coming from anthropogenic sources. The major factors affecting CO_2 injection are CO_2 availability and cost to build pipelines to carry CO_2 to oil fields (Jessen et al., 2005).

When CO_2 is injected at high pressure (miscible conditions), it vaporizes light components of the oil and then it condenses into the oil phase forming a single phase of CO_2 and oil. This single phase has low viscosity, enhanced mobility, low surface tension and reduces the density difference between oil and water, leading to more effective displacement. CO_2 miscible flooding may result in 15-65% of additional oil recovery (Mathiassen, 2003). It can extend the field life,

reduce the greenhouse gas emissions, and increase the profitability of the field. However, at the same time CO_2 has a number of reservoir engineering problems mainly formation damage and mobility control.

Reservoir depletion typically leads to phase separation and compositional change resulting in shifting of equilibrium conditions. It is also observed that when CO_2 is injected for EOR, it will change compositions and pH of oil leading to flocculation, precipitation, and deposition of organic solids mainly asphaltenes (Khurshid and Choe, 2014d).

Other common problems with CO_2 injection are gravity tonguing and viscous fingering (Civan, 2000). These problems are more severe in CO_2 flooding than in waterflooding, because CO_2 is lighter, less viscous and more mobile as compared to oil and water. This high mobility of CO_2 leads to low volumetric sweep efficiency during CO_2 flooding and is regarded as the main hurdle in achieving profitable CO_2 flooding.

The asphaltenes are high molecular weight, polar, and polyaromatic components of crude oil. They are soluble in toluene but insoluble in n-alkenes such as n-pentane or n-heptane. They are dark colored with a density of 1.2 g/cm^3 and are infusible meaning no defined melting point. Thus on heating, they decompose leaving carbonaceous residues (Mullins et al., 2007). The asphaltene deposition in a reservoir represents formation damages as it reduces the fluid volume and plugs pore throats. It can also trigger a change in wettability, and relative permeability shifts from a water wet to an oil wet system. Therefore, it affects flood performances (Mathiassen,

2003). Regarding the change in oil viscosity, asphaltene fines are considered as colloids in the oil phase. So when it precipitates, oil viscosity changes.

Wan et al. (2011) estimated that a reservoir fluid with just 0.067% asphaltene will lead to deposition of 90 kg of asphaltene after 1000 bbl of oil. Therefore, it is necessary to reduce asphaltene deposition in the reservoir to increase oil recovery. Its deposition in tubings and pipes is studied and a lot of remedies are proposed. Various methods include chemical, mechanical, thermal, external force, and biological methods. However, there is no reliable solution for asphaltene deposition in pores of an oil reservoir (Okwen, 2006).

Regarding the optimization of CO_2 injection and EOR, there are two main approaches: production optimization and computational optimization. A lot of work is done on different methods of CO_2 injection to increase oil recovery (Mathiassen, 2003; Jessen et al., 2005; Kovscek and Cakici, 2005; Okwen, 2006; Jahangiri and Zhang, 2011; Dai et al., 2013). At the same time much work is done on different techniques of computational optimization for low numeric effort (Kolda et al., 2003; Echeverria et al., 2011; Cameron and Durlofsky, 2012). All of them researched either production or computational optimization. However, there is dire need of coupled optimization to increase oil recovery and CO_2 storage, and to decrease asphaltene deposition (Khurshid and Choe, 2014d).

The objective of this study is to determine the amount of formation damages caused due to asphaltene deposition and problems faced in CO_2 injection activities. The goal is to propose

conditions such as depth, temperature, and fluids properties to minimize asphaltene concentration. The emphasis of this study is not only to minimize the deposition of asphaltene, but also to find certain conditions where the deposited asphaltene can be re-dissolved and removed from the reservoir.

After detail simulation study, an integrated methodology is developed. The methodology consists of detail analysis of different injection schemes for CO_2 to increase the recovery of oil and CO_2 storage, and to reduce the deposition of asphaltene. Fig. 5.1 shows the flowchart of the developed methodology.

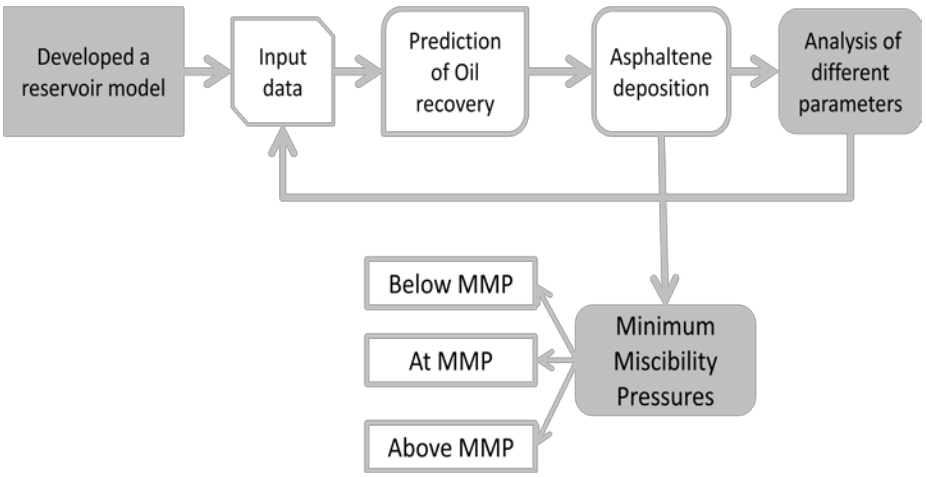

Fig. 5.1 Flowchart of the developed methodology.

5.2 Methodology of Optimization

In EOR projects, the goal is to maximize the profit by optimizing the oil recovery and CO_2 injection. This objective has been set to

- Increase oil recovery
- Decrease asphaltene deposition
- Decrease water production and injection
- Increase CO_2 injection
- Reduce CO_2 production
- Increase cumulative CO_2 storage
- Maximize oil recovery and CO_2 storage at the end of the flooding period

A detail study on CO_2 injection rate is performed with a commercial reservoir simulator to determine the effect of gas injection, oil recovery, gas storage, and asphaltene deposition in a reservoir. To simulate the asphaltene behavior a 1D model is used with ASPHALTE keyword in Eclipse-300 data file. In the model the asphaltene deposition is included to monitor the changes in the compositions of oil, pH of the media, and precipitation of asphaltene.

5.3 Validation and Comparison

With the developed methodology, a detail analysis is performed and a number of MMPs are determined, but three of them are important: near, at, and above MMP. For the first MMP asphaltene deposition is high. However, when the pressure is at, and above the MMP, the deposited asphaltene is removed from the reservoir leading to its re-dissolution.

To check the validity of the findings on asphaltene re-dissolution and removal, the results are also compared with works of Victorov and Firoozabadi (1996) and Tavakkoli et al. (2010). Victorov and Firoozabadi (1996) mentioned that at high concentration the number of asphaltene monomers decreases in the oil and some of the solid asphaltene will re-dissolve in the oil. Tavakkoli et al. (2010) after performing experiments on CO_2 injection for heavy crude, mentioned that asphaltene precipitation decreases when the mixture switches from bubble-point to a dew point fluid. These experimental data support and confirm the findings made in this study.

The results are compared with the experimental results of Hu et al. (2004): they showed that appreciable asphaltene was precipitated at pressures close and greater than MMP. They also mentioned that asphaltene precipitation increases with the increase of CO_2 and the asphaltene deposition increases at pressure close to MMP. However, it is found in this study that once MMP is crossed the concentration of asphaltene decreases and the deposited asphaltene is re-dissolved and removed from the reservoir as shown in Fig. 5.2.

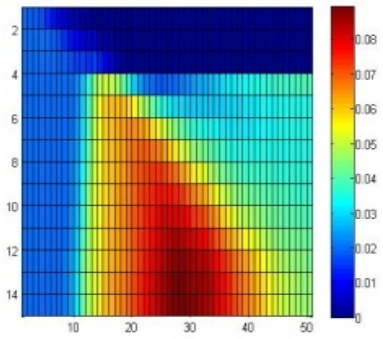

(a) 3000 Mscf/day close to MMP

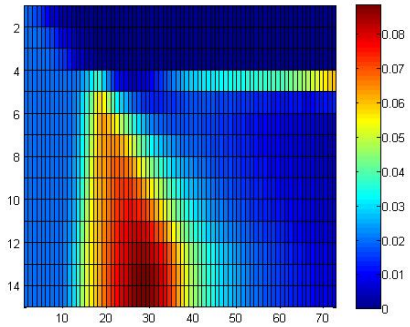

(b) 5000 Mscf/day at MMP

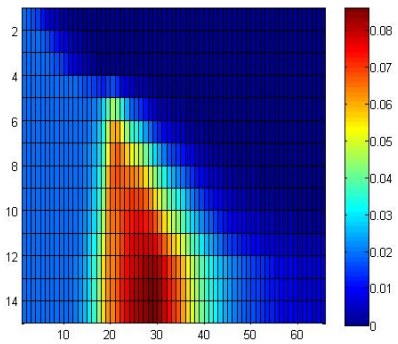

(c) 7000 Mscf/day above MMP

Fig. 5.2 Asphaltene deposition at different CO_2 injection rates.

To determine whether asphaltene deposition, redissolution and removal are due to pressure change or CO_2. A comparison is performed for asphaltene deposition with CO_2 flooding and waterflooding. CO_2 flooding and waterflooding was performed with same oil production rate (3500 bbl/day), reservoir temperature (50 ^oC), and rock properties.

It can be observed that asphaltene deposits with the oil production in the both cases in the same manner as shown in Fig. 5.3. On the other hand in waterflooding the asphaltene deposition is more and it remains at a concentration of 0.08% in the reservoir. However, in the CO_2 flooding the deposited asphaltene is re-dissolved and removed, and its concentration is reduced to 0.03% in the reservoir.

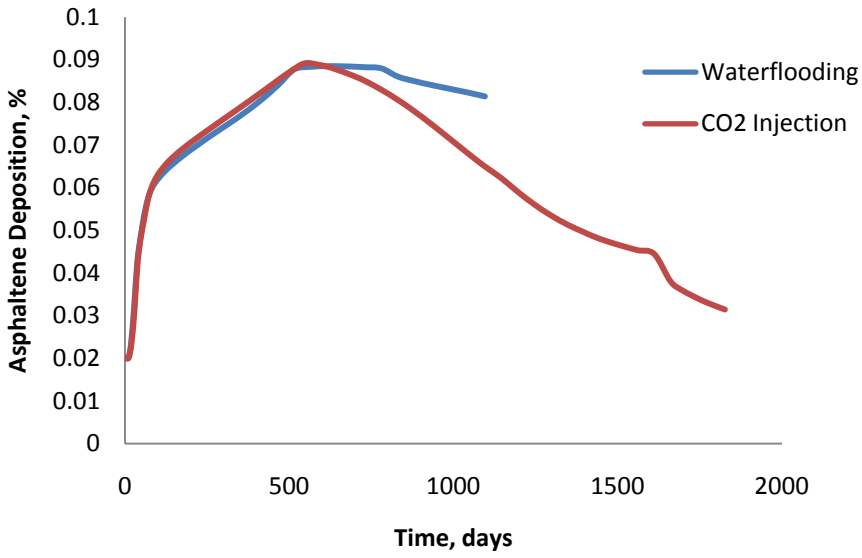

Fig. 5.3 Comparison of asphaltene deposition at CO_2 and water injection.

5.4 Factors Affecting Asphaltene Deposition

When oil is produced from a well, light components of oil are recovered and the concentration of the heavy components increases. Therefore, it will be accompanied by lesser amounts of C_2 to C_{12} components leading to phase separation. Also with the injection of CO_2, the changes in oil composition and pH, destabilize the equilibrium conditions. These phenomenon causes asphaltene deposition.

A detail sensitivity analysis of reservoir properties and injection parameters is performed to determine the effect of factors affecting asphaltene deposition. The different factors affecting asphaltene deposition are as follow.

5.4.1 Effect of CO_2 Injection Rate

CO_2 is typically not first-contact miscible with reservoir fluids. It forms multi-contact miscibility on mixing with reservoir fluids (Mathiassen, 2003) and thus attains miscibility step by step with a certain reservoir fluid at a time. This means that a greater mass of CO_2 would be required for mass transfer of component from multiple and repeated contact between oil and CO_2. This process is regarded as a major advantage of CO_2 miscible process to extract heavy hydrocarbons. However, to inject CO_2 at miscible conditions, it requires high pressure to compress the CO_2 and promote adequate enrichment at the displacement front.

Fig. 5.4 demonstrates oil production with time at different CO_2 injection rates at 1000, 3000, 5000, 7000, and 9000 Mscf. The oil production rate, reservoir temperature, asphaltene percentage were kept constant at 3500 bbl/day, 50 ^{o}C, and 0.02%, respectively, with homogenous rock properties. Short and long plateau of oil production can be observed. The short plateau represents immiscible condition at 1000 and 3000 Mscf/day. However, the longer one improves the oil production and illustrates that miscibility pressure has achieved in the reservoir at 5000, 7000, and 9000 Mscf. Hence, it is important to inject CO_2 at a certain injection rate to attain MMP, which will result in high oil recovery. MMP is a pressure above which an additional increase in pressure causes only a minimal increase in oil recovery. Therefore, it is apparent from the results that, MMP is 5000 Mscf.

The effect of increased CO_2 injection rates is also evident from Fig. 5.4. Once miscibility is reached, there are less benefits of injecting CO_2 at a higher rate. In other words, high injection rate will not increase recovery but will help to attain miscibility pressure and may result in early CO_2 breakthrough. If there is large pressure difference between the injector and the producer, gas goes faster towards the producer and less oil is recovered. If breakthrough occurs, injecting more CO_2 won't help much, it will go directly from the injector to the producer path. Therefore, an optimum injection rate should be selected to have high recovery and delayed breakthrough.

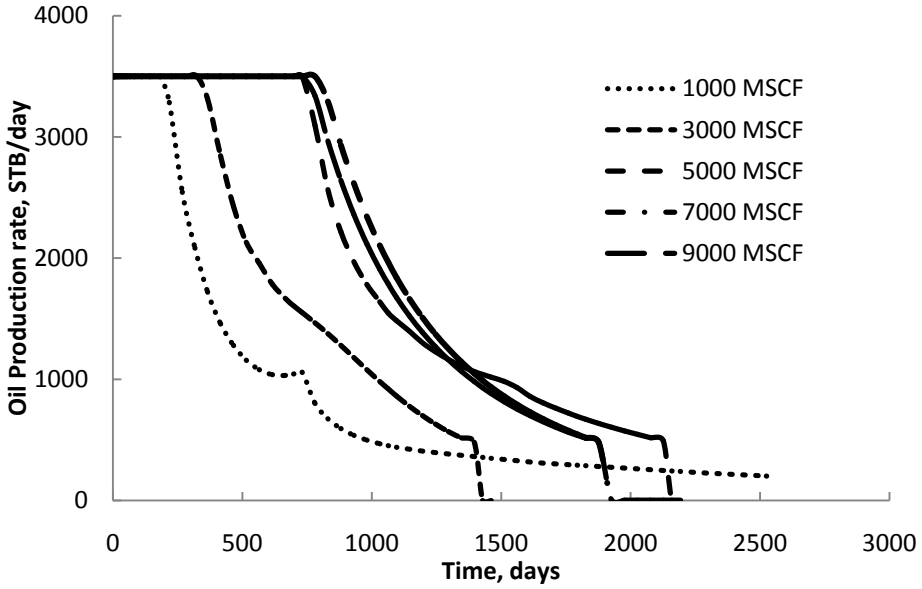

Fig. 5.4 Effects of CO_2 injection rate on oil recovery.

5.4.2 Effects of Immiscible and Miscible Pressures

Two injection rates 1000 and 5000 Mscf/day are analyzed to determine asphaltene deposition in the reservoir. As described above, injection rate of 1000 Mscf/day didnot achieve miscibility, while 5000 Mscf/day did.

Fig. 5.5 demonstrates that asphaltene deposition increases in both the cases from the very start. However, asphaltene deposition decreases after reaching a maximum point: This decrease is high at the miscible conditions while at the immiscible conditions the asphaltene concentration remains relatively constant.

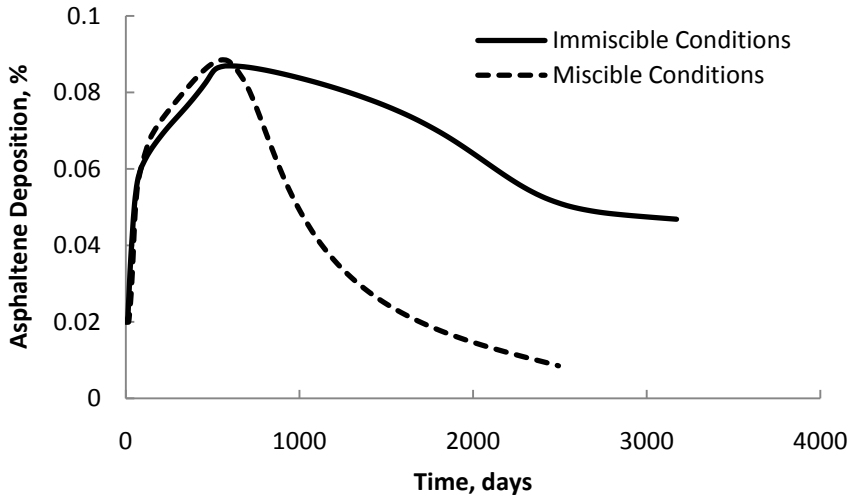

Fig. 5.5 Effects of immiscible and miscible pressures on asphaltene deposition.

A detail analysis is performed to determine the characteristics of maximum point of asphaltene deposition in the reservoir. Both asphaltene deposition and CO_2 break-through are plotted together for the immiscible and miscible cases. Fig. 5.6a shows the immiscible case while 5.6b is for the miscible case.

From the results it is obvious that CO_2 break-through defines the maximum point of asphaltene deposition in the reservoir. For immiscible conditions, when the injection operation has ended, the deposited asphaltene remains in the reservoir at high concentration. While at the miscible conditions the deposited asphaltene is reduced to the lowest point, because at high rate CO_2 develops contact with the deposited asphaltene. Thus at the miscible conditions CO_2 re-dissolves and removes the deposited asphaltene from the reservoir.

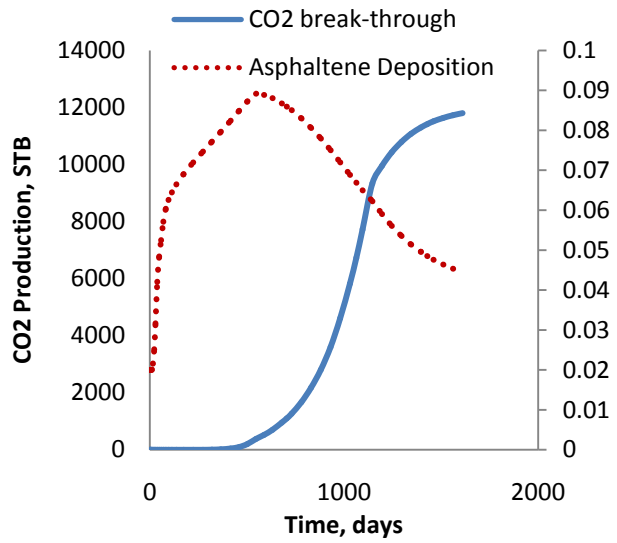

(a) immiscible condition (injection of 1000 Mscf/day)

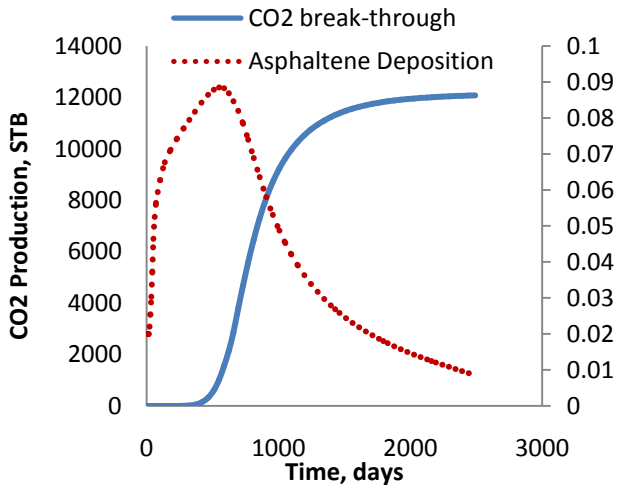

(b) Miscible conditions (injection of 5000 Mscf/day)

Fig. 5.6 Effects of different pressures on asphaltene deposition.

5.4.3 Effects of Different MMP

Five cases are selected to closely examine the effect of asphaltene deposition in the reservoir. These cases are below, near, at, above, and far from MMP. Fig. 5.7 shows the amount of asphaltene at these cases. 1000 Mscf/day is below MMP (immiscible conditions), 3000 Mscf/day near MMP, 5000 Mscf/day at MMP, 7000 Mscf/day above MMP, and 9000 Mscf/day far from MMP. With oil production rate, reservoir temperature, asphaltene percentage kept constant at 3500 bbl/day, 50 ^{o}C, and 0.02%, respectively.

The results in Fig. 5.7 demonstrate that, in all cases there is asphaltene depositions because pressure depletion and CO_2 injection typically leads to phase separation and compositional change. As a result, asphaltene deposition cannot be stopped. However, when CO_2 is injected at, above, and far from the MMP, we will have very low 0.01% asphaltene remaining in the reservoir at the end of the operation (deposited asphaltene is removed).

Further analysis of injection parameters shows that a point in range between at and above MMP should be selected, where recovery of oil and CO_2 storage is high with low CO_2 injection rate (less operating cost). This practice results in maximum oil recovery and CO_2 storage, but will reduce asphaltene concentration in the reservoir.

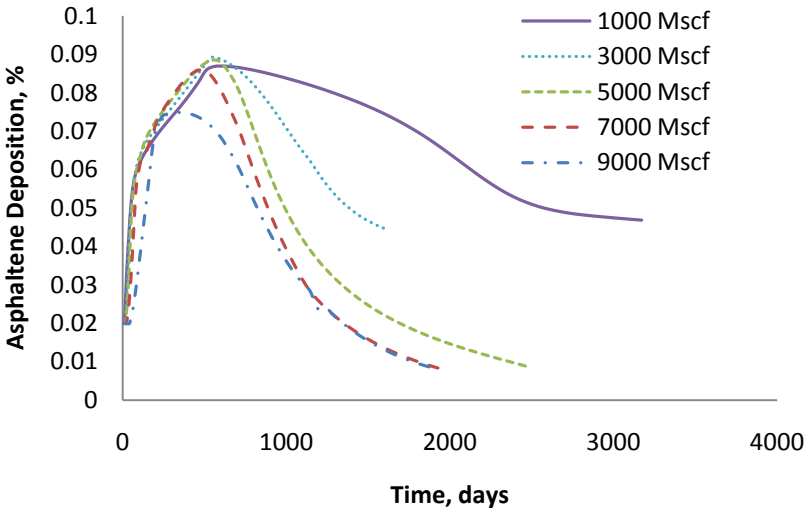

Fig. 5.7 Effect of different MMP on asphaltene deposition.

5.4.4 Effects of Heterogeneities

From the analysis of different factors affecting asphaltene deposition. It is found that the rock properties have a great influence on asphaltene deposition and formation damage. It is observed that the CO_2 injection pressure depends on the permeability and reservoir thickness. Takahashi et al. (2003) mentioned that due to size of pore throat, connectivity of pore and rock heterogeneity a crude oil with more than 17.2 wt% asphaltene may not represent asphaltene problem, however crude oil with < 0.1% could pose serious problem.

A number of simulations are performed to determine the effect of different rock heterogeneities and to know the effect of variation in permeability and porosity. The CO_2 injection rate, oil production rate, reservoir temperature and asphaltene percentage

were kept constant at 5000 Mscf/day, 3500 bbl/day, 50 ^{o}C, and 0.02%, respectively. When the rock properties are assumed homogenous throughout the reservoir, the deposition of asphaltene is low as evident from Fig. 5.8a. However, when the rock properties are heterogeneous (given stochastically), the amount of asphaltene deposition increases (Fig. 5.8b).

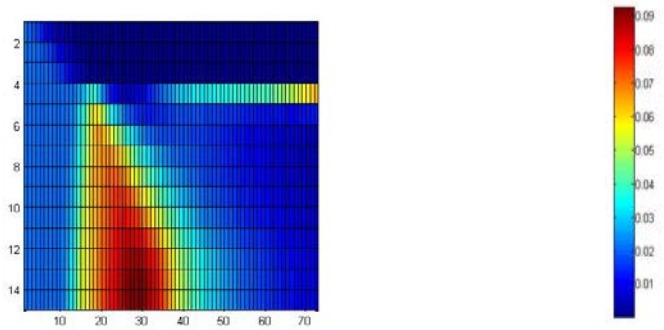

(a) Homogenous porosity and permeability

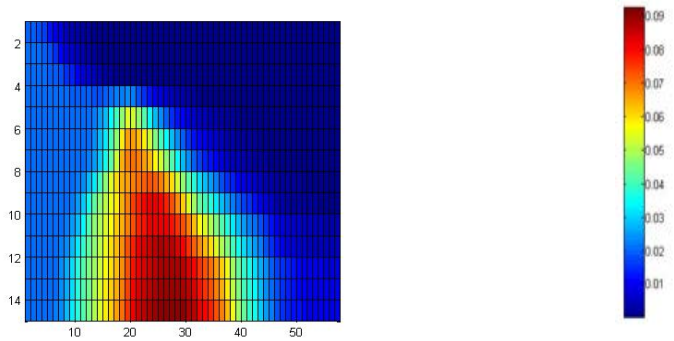

(b) Heterogeneous porosity and permeability case.

Fig. 5.8 Effects of different heterogeneities on asphaltene deposition.

5.4.5 Effects of Asphaltene Percentage in Oil

Fig. 5.9 illustrates the effect of asphaltene percentage in the oil. The following properties were kept constant: CO_2 injection rate at 5000 Mscf/day, oil production rate at 3500 bbl/day, reservoir temperature at 50 ^oC, with homogenous rock properties. When the percentage of asphaltene is 0.02% in the oil, the amount of asphaltene deposition will be low as shown in Fig. 5.9a. However, when its amount increases from 0.02 to 0.04%, asphaltene deposition also increases. Therefore, before starting CO_2 injection it is very important to know the reservoir fluid compositions, amount, and percentage of heavy components of oil. This practice will help to take necessary action to reduce asphaltene deposition.

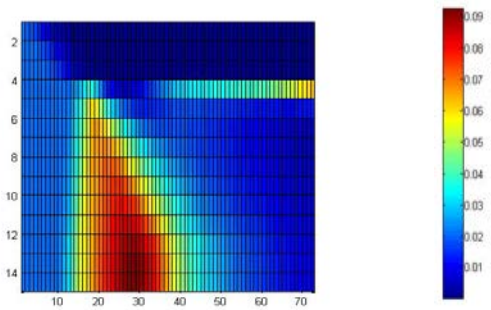

(a) 0.02% asphaltene

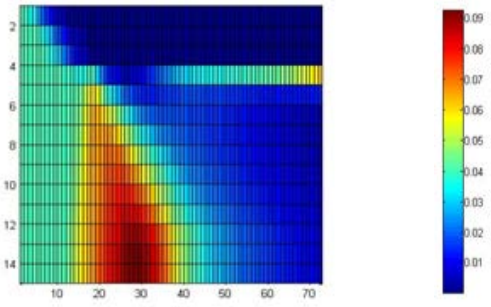

(b) 0.04% asphaltene

Fig. 5.9 Effects of asphaltene percentage in oil.

5.5 Summary

1. Reservoir depletion typically leads to phase separation, compositional change, and shifting of equilibrium conditions. When CO_2 is injected for EOR, it will change compositions and pH of oil leading to flocculation, precipitation, and deposition of asphaltenes. This asphaltene reduces the fluid volume and plugs pore throats. Its deposition can also change wettability and relative permeability.
2. It is found that different factors affecting asphaltene deposition are properties of host rock (heterogeneities), composition of formation fluids, the thermodynamic conditions, and flow rate. The developed scheme in this study reduced the typical problems faced by the industry and can be used to monitor the dynamic behavior of CO_2, and will help to control the drawbacks of CO_2 injection.
3. It is found that, when the conditions are miscible, recovery increases but it also triggers asphaltene deposition. For a number of MMPs three of them are important: near, at, and above MMP. For the first MMP asphaltene is high. However, when the pressure is at and above the MMP, the deposited asphaltene is removed from the reservoir. The reason is that CO_2 develops contact with asphaltene at high pressure leading to its re-dissolution and removal.

Chapter 6

CONCLUSIONS AND RECOMMENDED FUTURE WORK

This chapter summaries the development of the reservoir compaction model in Chapter 2, development of the thermal model for CO_2 temperature prediction in Chapter 3, development of the formation damage model in Chapter 4, and methods to minimize asphaltene related damages in Chapter 5. In addition, it recapitulates the major arguments put forth in this dissertation and suggests areas for future research.

Reservoir Compaction

In this study an analytical model is derived to predict reservoir compaction by considering the arrangement of pores at macroscopic scale in a reservoir rock. On the basis of the model a failure line methodology is developed to determine minimum reservoir pressure and an optimal time ranges for CO_2 injection to enhance CO_2 storage and oil recovery. Thus, it is suggested to inject CO_2 in a reservoir before touching the failure line, which can easily be determined using the proposed method. The developed model and the failure-line methodology can be used to investigate and predict the effect of pressure depletion, reservoir compaction, the critical pore collapse stress point, and an optimal time ranges for CO_2 injection.

The proposed methodology is validated with experimental as well as field data available. A good agreement between the predicted

pore collapse behavior and the field data proves the accuracy of our work. Further, this study has revealed key insights into the reservoir compaction, which depends on the pressure, production rate, porosity, and geometry of the pores. Understanding these factors will be critical for determining the dynamic geomechanical behavior of the reservoir rock easily and cost effectively.

CO_2 Thermal Model

In the present study, a simulator is developed to predict accurate temperature of CO_2, and thermal disturbances. It helps to control dynamic behaviors of injected CO_2. The developed simulator uses experimental determined specific heat values of CO_2 to predict accurate thermal disturbances and dynamic behaviors of injected CO_2 for handling its injection performances, in shallow or deep reservoirs.

The thermal and chemical impacts of CO_2 injection can be minimized by controlling CO_2 injection rate, time, and its surface temperature. From the CO_2 reactive modeling, it is evident that the porosity increases significantly in the near wellbore region due to dissolution. It is also illustrated that temperature of CO_2 and its injection rate control the mineral precipitation and spatial reactivity in a reservoir. It is observed that deep oil and gas reservoirs are good candidates for CO_2 sequestration than shallow reservoirs because of low formation damages.

Formation Damage Model

In this work a comprehensive model is developed that solves fluid flow equations, chemical reactivity equations, and particles deposition equations. The developed model also encircles the cementation of asphaltene and carbonate particles, and the change in porosity due to cementation. The model is validated with experimental data available and predicts the total extent of formation damages due to CO_2-rock-water-oil interactions. It is observed that the consequences of asphaltene and carbonate precipitation are severe and may lead to irreversible formation damages specifically cementation. This cementation may cause permanent pore blockage leading to reduction of oil and gas productivity and CO_2 injectivity.

In this study, it is found that the dissolution rate is high in shallow and heterogeneous formations, because low temperature conditions accelerate rock dissolution and deposition processes. On the other hand, high reservoir temperature causes an increase in the solubility of organic and inorganic particles leading to less damage. Therefore, deep reservoirs are more competitive than shallow reservoirs for CO_2 sequestration. Thus, the developed formation damage simulator can be used as an effective tool to control the formation damages giving maximum oil recovery and CO_2 storage.

Methods to Minimize Damage

Reservoir depletion and CO_2 injection typically cause phase separation and compositional changes resulting in shifting of equilibrium conditions and pH of oil. These processes may lead to flocculation, precipitation, and deposition of organic solids mainly asphaltenes. It is found that different factors affecting asphaltene deposition are properties of host rock (heterogeneities), composition of formation fluids, the thermodynamic conditions, and flow rate. The developed scheme in this study reduces typical problems faced by the industry and can be used to monitor the dynamic behavior of CO_2, and will help to control the disadvantages of CO_2 injection.

It is found that, when the conditions are miscible, recovery increases but it also triggers asphaltene deposition. For a number of MMPs three of them are important: near, at, and above MMP. For the first MMP asphaltene deposition is high. However, when the pressure is at and above the MMP, the deposited asphaltene is removed from the reservoir. The reason is that CO_2 develops contact with asphaltene at high pressure leading to its re-dissolution and removal.

FUTURE WORK ON CO_2 EOR

The fields of CO_2 EOR and CCS are growing because they may be the only commercial solution to mitigate CO_2 emissions and enhanced oil recovery. CO_2 EOR can be applied at any time during oil production life but more work is needed to increase its chances of successful application. Further research will improve the understanding of CO_2 EOR within the areas of rock compaction, CO_2 injection time, CO_2 thermal modeling, CO_2 related formation damages, and methods to minimize these damages. On the basis of the conclusions, the following are the many issues that should be addressed in future research.

- Experimental investigation of asphaltene deposition, rock dissolution/precipitation, and their cementation. Such experimental study is needed to have a true picture of formation damages during CO_2 injection activities in depleted reservoirs.
- Determination of formation damages at different CO_2 temperature such as hot and cold CO_2 in a laboratory with conditions mimicking reservoir conditions.
- Laboratory scale core study to optimize the oil recovery and CO_2 storage and to minimize asphaltene deposition in porous media.

References

Aadnoy, B.S. 1991. Effects of Reservoir Depletion on Borehole Stability. Journal of Petroleum Science and Engineering 6, 57-61.

Addis, M.A. 1997. Reservoir Depletion and its Effect on Wellbore Stability Evaluation. International Journal of Rock Mechanics and Mining Sciences 34, 401-417.

André, L., Azaroual, M. and Menjoz, A. 2009. Numerical Simulations of the Thermal Impact of Supercritical CO_2 Injection on Chemical Reactivity in a Carbonate Saline Reservoir. Transport in Porous Media 82, 247-274.

André, L., Audigane, P., Azaroual, M., and Menjoz, A. 2007. Numerical Modeling of Fluid rock Chemical Interactions at the Supercritical CO_2 - Liquid Interface during CO_2 Injection into a Carbonate Reservoir, The Dogger Aquifer (Paris Basin, France). Energy Conservation and Management 48, 1782-1797.

Apak, E.C. and Ozbayoglu, E.M. 2009. Heat Distribution within the Wellbore While Drilling. Petroleum Science and Technology 27, 678-686.

Arnold, F.C. 1990. Temperature Variation in a Circulating Wellbore Fluid. Journal of Energy Resources 112, 79-83.

Bacci, B., Korre, A., and Durucan, S. 2011. An Experimental and Numerical Investigation into the Impact of Dissolution/Precipitation Mechanisms on CO_2 Injectivity in the Wellbore and Far Field Regions. International Journal of Greenhouse Gas control 5, 579-588.

Bloomberg. 2012. Carbon capture and storage: Research note, Bloomberg New Energy Finance 27 June.

Cameron, D.A., and Durlofsky, L.J. 2012. Optimization of Well Placement, CO_2 Injection rate, brine cycling for geological Carbon Sequestration. International Journal of Greenhouse Gas Control 10, 100-112.

Civan, F. 2000. Reservoir Formation Damage Fundamentals, Modeling, Assessment, and Mitigation. First edition, Gulf Publishing Company, Houston, Texas.

Corzo, M.M., MacBeth, C., and Barkved, O. 2013. Estimation of Pore Pressure Change in a Compacting Reservoir from Time-Lapse Seismic Data. Geophysical Prospecting 61 (5), 1022-1034.

Dai, Z., Middleton, R., Viswanathan, H., Rahn, J.F., Bauman, J., Pawar, R., Lee, S.Y., and Mcpherson, B. 2013. An Integrated Framework for Optimizing CO_2 Sequestration and Enhanced Oil Recovery. Environmental Science and Technology Letters 1, 49-54.

Davies, J.P., and Davies, D.K. 2001. Stress Dependent Permeability: Characterization and Modeling. SPE 71750. SPE Journal 6, 224-235.

Dulov, V. 2011. Simulation of CO_2 Injectivity in a Laboratory Cylindrical-Cone Model. MS-thesis. University of Stavanger.

Echeverria. C.D., Isebor, O., and Durlofsky, L. 2011. Application of Derivative Free Methodologies to Generally Constrained Oil Production Optimization Problems. International Journal of Mathematical Modeling and Numerical optimization 2 (2), 134-161.

Foulkes, F.R. 2013. Physical Chemistry for Engineering and Applied Sciences. CRC Press Taylor & Francis Group, Florida. USA.

Gruesbeck, C., and Collins, R.E. 1982. Entrainment of Deposition of Fine Particles in Porous Media. SPE Journal 22 (6), 847–856.

Gaus, I., Audigane, P., André, L., Lions, J., Jacquemet, N., Durst, P., Czernichowski-Lauriol, I., and Azaroual, M. 2008. Geochemical and Solute Transport Modeling for CO_2 Storage, What to Expect from it?. International Journal of Greenhouse Gas Control 2, 605-625.

Geertsma, J., 1973. Land Subsidence above Compacting Oil and Gas Reservoirs. Journal of Petroleum Technology 734-744.

Global CCS Institute, 2012. The Global Status of CCS: 2012. Global CCS Institute, Canberra, Australia.

Godec, M. 2011. Global technology roadmap for CCS in industry: Sectoral assessment CO_2 enhanced oil recovery, prepared by Advanced Resources International for United Nations Industrial Development Organization (UNIDO).

Hasan, A.R. and Kabir, C.S. 2002. Fluid Flow and Heat Transfer in Wellbores, SPE Richardson, Texas.

Hillis, R.R. 2000. Pore Pressure /Stress Coupling and its Implications for Seismicity. Exploration Geophysics 31, 448-454.

Hu, Y.F., Li, S., Liu, N., Chu, Y.-P., Park, S.J., Mansoori, G.A., and Guo, T.M. 2004. Measurement and Corresponding States Modeling of Asphaltene Precipitation in Jilin Reservoir Oils. Journal of Petroleum Science and Engineering 41, 169-182.

IEA. 2012. Global carbon-dioxide emissions increase by 1.0 Gt in 2011 to record high. News item, 24 May, OECD/IEA. http://www.iea.org/newsroomandevents.

Intergovernmental Panel on Climate Change (IPCC). 2005. In: Metz et al.(Eds.). http:// www.mnp.nl-ipcc.

Izgec, O., Demiral, B., and Bertin, H. 2006. Experimental and Numerical modeling of Direct Injection of CO_2 into Carbonate Formations. Paper SPE 100809. SPE Annual Technical Conference and Exhibition held in San Antonio, Texas, USA on 24-27 September.

Jaeger, J.C., Cook, N.G.W., and Zimmerman, R.W. 2007. Fundamentals of Rock Mechanics. Blackwell Publishing, Oxford, UK.

Jahangiri, H.R., and Zhang, D. 2011. Optimization of the Net Present Value of Carbon Dioxide Sequestration and Enhanced Oil Recovery. Paper OTC 21985. Offshore Technology Conference held in Houston, Texas, USA on 2-5 May.

Jessen, K., Kovscek, A.R., and Orr Jr, F.M. 2005. Increasing CO_2 Storage in Oil Recovery. Energy Conversion and Management 46 (293), 293-311.

Khurshid, I., Fujii, Y., and Choe, J. 2014a. Analytical Model to Determine CO_2 Injection Time in a Reservoir for Optimizing its Storage and Oil Recovery: A Reservoir Compaction Approach. Submitted to International Journal of Rock Mechanics and Mining Sciences.

Khurshid, I., and Choe, J. 2014b. Analysis of Carbon dioxide Temperature, its Thermal Disturbance and Evaluating the Formation Damages during its

Injection in Shallow, Deep and High Temperature Reservoirs. Submitted to International Journal Oil, Gas and Coal Technology.

Khurshid, I., and Choe, J. 2014c. Analyses of Asphaltene and Carbonate Precipitation in Depleted Reservoirs during CO_2 Injection. Submitted to Greenhouse Gases: Science and Technology.

Khurshid, I., and Choe, J. 2014d. An Integrated Methodology to Optimize CO_2 Storage and Oil Recovery, and to Reduce Asphaltene Deposition during CO_2 Based EOR. Paper SPE 171103. SPE Heavy and Extra Heavy Oil Conference: Latin America Medellin Colombia, 24-26 September.

Khurshid, I., Lee, K.J., and Choe, J. 2013. Analyses of Thermal Disturbance in Drilling Deep and High Temperature Formations. Energy Sources, Part A: Recovery, Utilization, and Environmental Effects 35 (16), 1487-1497.

Khurshid, I. and Choe, J. 2013. Characterizing Formation Damages due to Carbon Dioxide Injection in High Temperature Reservoirs and Determining the Effect of Solid Precipitation and Permeability Reduction on Oil Production. Paper SPE 165158. SPE European Formation Damage Conference and Exhibition held in Noordwijk, Netherlands, 5-7 June.

Khurshid, I., Lee, K.J., Bahk, J.J., and Choe, J. 2010. Heat Transfer and Well Bore Stability Analysis in Hydrate Bearing Zone in the East Sea, South Korea. Paper SPE 20582. Offshore Technology Conference (OTC) held in Houston, Texas USA, 3-6 May.

Khurshid, I., Lee, K.J., Bahk, J.J., and Choe, J. 2010. Subsurface Temperature Model for Simulating Down hole Thermal Conditions during Drilling and its Validation. KSGE Conference held in Jeju South Korea, 6-7 May.

Kolda, T., Lewis, R., and Torczon, V. 2003. Optimization by direct search: new perspectives on some classical and modern methods. SIAM Review 45(3), 385-482.

Kovscek, A.R, and Cakici, M.D. 2005. Geologic Storage of Carbon Dioxide and Enhanced Oil recovery II. Cooptimization of Storage and recovery. Energy Conversion and Management 46, 1941-1956.

Lake, W.L. 1989. Enhanced Oil Recovery. Prentice Hall, Inc., New Jersey, USA.

Matter, J.M. and Kelemen, P.B. 2009. Permanent Storage of Carbon Dioxide in Geological Reservoirs by Mineral Carbonation. Nature Geoscience 2, 837-841.

Mathiassen, O. M., 2003. CO_2 as Injection Gas for Enhanced Oil Recovery and Estimation of the Potential on the Norwegian Continental Shelf, Part I of II. Norwegian University of Science and Technology.

Meyer, J.P., 2007. Summary of Carbon dioxide Enhanced Oil Recovery Injection Well Technology. American Petroleum Institute, 54.

Mullins, O.C., Sheu, E.Y., Hammami, A. and Marshall, A.G. 2007. Asphaltenes, Heavy Oils and Petroelomics. New York City: Springer.

Okwen. R.T. 2006. Formation Damage by CO_2-Induced Asphaltene precipitation. Paper SPE 98180. SPE International Symposium and Exhibition on Formation Damage Control held in Lafayette, LA, 15-17 February.

Ramey, H.J. 1962. Wellbore Heat Transmission. Journal of Petroleum Technology 14, 427-435.

Romero, J. and Touboul, E. 1998. Temperature Prediction for Deepwater Wells: A Field Validated Methodology. Paper SPE 49056. SPE Annual Technical Conference and Exhibition, New Orleans, 27-30 September.

Rutqvist, J., Birkholzer, J.T., and Tsang, C.F. 2008. Coupled Reservoir-Geomechanical Analysis of the Potential for Tensile and Shear Failure Associated with CO_2 Injection in Multilayered Reservoir-Cap Rock Systems. International Journal of Rock Mechanics and Mining Science 45, 132-143.

Schutjens, P.M., Snippe, J.R., Mahani, H., Turner, J., Ita, J., and Mossop, A.P., 2012 Production-Induced Stress Change in and above a Reservoir Pierced by Two Salt Domes: A Geomechanical Model and its Applications. SPE 131590. SPE Journal 17 (1), 80-97.

Segall, P., 1989. Earthquakes Triggered by Fluid Extraction. Geology 17, 942-946.

Settari, A., 2002. Reservoir Compaction. SPE 76805. Journal of Petroleum Technology 54 (8), 62-69.

Smits, R.M.M., de-Waal, J.A., and Kooten, J.F.C., 1988. Prediction of Abrupt Reservoir Compaction and Surface Subsidence Caused by Pore Collapse in Carbonates. SPE 15642. SPE Formation Evaluation, 3, 340-346.

Sharma, M.M., Yortsos, Y.C., and Handy, L.L. 1985. Release and Deposition of Clays in Sandstone. Paper SPE 13562. International Symposium on Oilfield and Geothermal Chemistry held in Phoenix, Arizona, on 9-11 April.

Soulgani, S.B., Tohidi, B., Ahmadi, J.M., and Rashtchian, D. 2011. Modeling Formation Damage due to Asphaltene Deposition in the Porous Media. Energy & Fuels 25, 753-761.

Srivastava, R.K., Huang, S.S., and Dong, M. 1999. Asphaltene Deposition during CO_2 Flooding. SPE Production and Facilities 14 (4), 235−245.

Takahashi, S., Hayashi, Y., Takahashi, S., Yazawa,N., and Sarma,H. 2003. Characteristics and Impact of Asphaltene Precipitation during CO_2 Injection in Sandstone and Carbonate Cores: An Investigative Analysis through Laboratory Tests and Compositional Simulation. Paper SPE 84895. SPE International Improved Oil Recovery Conference in Asia Pacific held in Kaula Lumpur Malaysia, 20-21 October.

Tavakkoli, M., Kharrat, R., Masihi, M., and Ghazanfari, M.H. 2010. Prediction of Asphaltene Precipitation during Pressure Depletion and CO_2 Injection for Heavy Crude. Petroleum Science and Technology 28(9), 892-902.

Tans, P. 2014. NOAA/ESRL (www.esrl.noaa.gov/gmd/ccgg/trends/) and Keeling, R. 2014. Scripps Institution of Oceanography (scrippsco2.ucsd.edu/).

Teufel, L.W., Rhett, D.W., and Farrell, H.E. 1991. Effect of Reservoir Depletion and Pore Pressure Drawdown on In-situ Stress and Deformation in the Ekofisk Field, North Sea. Rock Mechanics as a Multidisciplinary Science, In: Rogiers, J.C. (ed.), Balkema, Rotterdam, 63-72.

Vicotorov, A.I., and Firoozabadi, N.A. 1996. Thermodynamics of Asphaltene Precipitation in Petroleum Fluids by a Micellization Model. American institute of Chemical Engineers Journal 42, 1753-1764.

Wang, J., Ryan, D., Anthony, E.J., Wildgust, N., and Aiken, T. 2011. Effects of Impurities on CO_2 Transport, Injection and Storage. Energy Procedia 4, 3071-3078.

Wang, S., and Civan, F. 2001. Productivity Decline of Vertical and Horizontal Wells by Asphaltene Deposition in Petroleum Reservoirs. Paper SPE 64991-MS. SPE International Symposium on Oilfield chemistry held in Houston, Texas, USA on 13-16 February.

White, S.P., Allis, R.G., Moore, J., Chidsey, T., Morgan, C., Gwynn, W., and Adams, M. 2005. Simulation of Reactive Transport of Injected CO_2 on the Colorado Plateau, Utah, USA. Chemical Geology 217, 387-405.

Wan, N.A., Wan A.W.D., Nasir, D., Memom, A., Khan, A.I., and Jamaluddin, A. 2011. A Systematic Approach to Evaluate Asphaltene Precipitation during CO_2 Injection. Paper SPE No. 143903. SPE Enhanced Oil Recovery Conference held in Kuala Lumpur, Malaysia, 19-21.

Wark Jr., K. and Richards, D.E. 1999. Thermodynamics, 6th ed. McGraw-Hill, New York.

White, S.P., Allis, R.G., Moore, J., Chidsey, T., Morgan, C., Gwynn, W., and Adams, M. 2005. Simulation of Reactive Transport of Injected CO_2 on the Colorado Plateau, Utah, USA. Chemical Geology 217, 387-405.

Xiao, Y., Xu, T., and Pruess, K. 2009. The Effects of Gas-Fluid-Rock Interactions on CO_2 Injection and Storage: Insights from Reactive Transport Modeling. Energy Procedia 1, 1783-1790.

Yong, Z. and Renxuan, T. 2007. Study of Distribution of Wellbore Pressure and Temperature of CO_2 Injection Well. Offshore Oil 2, 59-64.

Zanganeh, P., Ayatollahi, S., Alamdari, A., Zolghadr, A., Dashti, H., and Kord, S. 2012. Asphaltene Deposition during CO_2 Injection and Pressure Depletion: A Visual Study. Energy & Fuels 26, 1412−1419.

Zeidouni, M., Pooladi-Darvish, M., and Keith, D. 2009. Analytical Solution to Evaluate Salt Precipitation during CO_2 Injection in Saline Aquifers. International Journal of Greenhouse Gas Control 3, 600–611.

Zhang, J., Wong, T.F., and Daniel, M.D. 1990. Micromechanics of Pressure-Induced Grain Crushing in Porous Rocks. Journal of Geophysical Research 95, 341-352.

Zhu, W., and Wong, T.F. 1997. The Transition from Brittle Faulting to Cataclastic Flow: Permeability Evolution. Journal of Geophysical Research 102, 3027-3041.

Zoback, M.D., 2007. Reservoir Geomechanics. Cambridge University Press, Cambridge. UK.

국문초록

본 논문에서는 석유가스의 증진회수 및 CO_2저장을 위한 새로운 방법을 연구하였다. 이를 위해 EOR 과 CO_2 주입 시간, CO_2열 모델링, CO_2 관련 지층 손상, 최적화 사이의 관계에 대한 연구를 수행하였다.

먼저 저류층에 CO_2를 주입하는 시간을 결정하기 위해 거시적 관점에서 저류층 내 공극을 격자시스템으로 모델링하였다. 이를 바탕으로 failure-line 압축예측 방법론을 이용하여 회복 불가능한 공극 붕괴 및 저류층 압축을 야기하는 임계응력을 구하였다. Failure-line 에 도달하는 시간을 계산하면 최적의 CO_2 주입시간을 결정할 수 있다. 그 결과 failure-line 에 도달하기 이전에 CO_2를 주입하는 것이 최적의 결과를 얻을 수 있음을 알게 되었다. 임계응력 이전까지 CO_2를 주입하면 석유가스 회수 및 CO_2 저장능력을 높일 수 있다.

유정에서 CO_2 온도변화와이에 영향을 미치는 인자들, 그리고 가열된 CO_2에 의해 야기된 지층손상에 대해 분석하였다. 이를 위해 시뮬레이터를 개발했으며, CO_2의 온도를 예측하기 위해 실험적으로 결정된 CO_2의 비열 값을 사용하였다. CO_2의 열역학적 성질은 온도 및 압력에 따라 변화하기때문에, 이 방법을 이용하면 정확한 CO_2 온도예측이 가능하다. CO_2 주입 변수들에 대한 민감도분석 결과 지열구배, 주입 속도, 표면 온도가 CO_2 격리 과정에서 CO_2의 온도를 조절하는 데 중요한 인자임을 알 수 있었다.

저류층에 CO_2를 주입할 때 물, 석유, 암석과 화학반응을 일으킨다. 이런 작용은 암석 용해, 아스팔트 침착, 탄산염 침전

등의 지층손상을 야기한다. 따라서 본 연구에서는 CO_2 관련 지층손상과 그 결과에 대해 분석하였다. 이를 위해 화학반응성, pH 변화, 아스팔트 침착, 입자의 용해·이동·침전을 모사하는 시뮬레이터를 개발했다. 분석 결과, 회복 불가능한 손상과 영구적인 폐색을 야기하는 교결현상이 다공성 매질에 발생했다. 이러한 현상은 아스팔트의 반응성과 양 그리고 CO_2의 암석과 물에 대한 반응성에 따라 영향을 받는 것으로 나타났다. 또한 CO_2 주입 속도가 높고 주입 시간이 길 때, 이러한 작용이 활발하게 발생하는 것으로 나타났다. 민감도분석으로부터 심도가 깊은 저류층이 낮은 저류층보다 CO_2 저장에 있어서 더 적은 지층손상을 보였다. 이를 통해 심도가 깊은 저류층이 CO_2 저장소로서 가장 적합한 후보라는 것이 입증되었다.

본 연구의 최종 목적은 CO_2 저장과 석유가스 회수를 최적화하면서 아스팔트 침착을 최소화하기 위한 통합된 방법론을 개발하는 것이다. CO_2가 비혼합 조건에서 주입 할 때, 낮은 회수율과 함께 아스팔트 침착 적게 발생한다. 반면, 혼합조건일 때는 회수율은 증가했지만, 아스팔트 침착 또한 촉진되었다. 세부분석을 통해 많은 최소혼화성압력(Minimum miscibility pressure, MMP)를 발견하였는데 그 중 MMP 이상의 압력이 중요한 것을 알 수 있었다. MMP 이상의 압력일 경우에는 저류층 내 고온의 아스팔트와 CO_2가 만나 침착된 아스팔트를 재용해시킨 후 제거된다.

주요어 : 저류층 압축, CO_2 주입, 최적시간 범위, 열모델링, 지층손상

학 번: 2011-31311